ISSN 1016-3115

wgn

30-4
august 2002

bimonthly journal of the international meteor organization

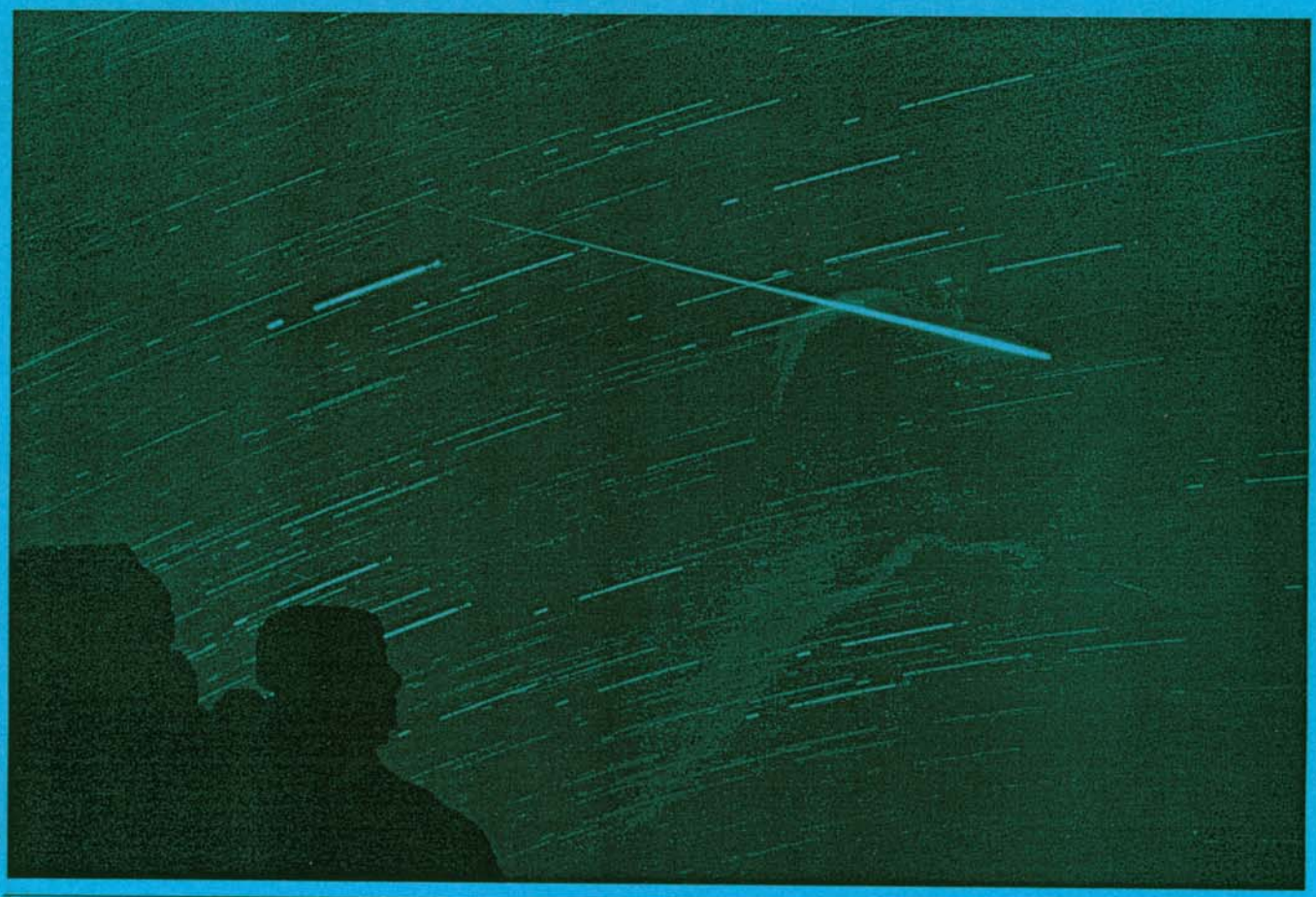

A bright Leonid meteor captured by Kun Zhou from Shandong, China, during the meteor storm of November 18, 2001, caused by the 4-revolution dust trail of Comet Tempel-Tuttle over Asia. The exposure lasted from 18^h30^m to 18^h50^m UT and was interrupted by clouds. The fireball moved from Canis Major to Lepus. Another faint meteor is barely visible in Columba.

In this issue:

In case of non-delivery, return postage guaranteed. Please return to:
v.u.: Marc Gyssens, Heerbaan 74, B-2530 Boechout, Belgium

WGN, Vol. 30, No. 4, August 2002, pp. 83–128

Contents

Useful Information

The October issue *(WGN 30:5)*

The Journal offers the unique chance to publish a wide range of articles—from high-end particle simulations to useful observing experiences. Remember that the success of meteor science, very obvious recently in connection with the Leonids, is based on the combination of amateur and professional work. A personal description of observing experiences is as much required as a prediction of a Leonid meteor storm! The *October issue* will be edited in the beginning of October 2002. Contributions should be sent to *Marc Gyssens* before September 10.

Subscriptions and ordering of publications

Volume 30 (2002) of *WGN* is expected to contain at least 240 pages and costs 20 EUR, including non-airmail delivery. Ordering other *IMO* publications is done in the same way as paying subscription/membership fees. Changes of address and complaints about not receiving *WGN* should be addressed to the Treasurer, Ina Rendtel.

All addresses can be found on the inside of the back cover.

Instructions for Authors Contributing to WGN

Rainer Arlt

1. The makings of WGN

Word-processing software typically shows on the screen what you will get out of the printer. Producing a text is reasonably possible with such software. A scientific magazine however requires good typographic quality also for formulae and technical symbols. This is achieved by the type-setting system TEX, which works with type-setting commands rather than with software functions applied to the text instantaneously. The TEX-compiler translates the text with commands into a printable document *after* the article has been written. This is the way *WGN* is made from your contributions.

Once you send a paper to *WGN*, the TEX commands are added to the text by the editor. The time needed to process your contribution depends on the complexity of the contents (formulae, tables, figures). The type-setting system formats the text according to general rules of book printing. This is why *you do not have to bother with your personal formatting* such as aligning the paragraphs and figures nicely etc. Insert a bit of *WGN's formatting instead!*

A few simple considerations will speed up the process of editing the Journal significantly. In the following Section, we will give a number of type-setting commands, which you can include in your article. It does not matter whether you have access to the TEXtype-setting package; if you send your article including these commands, you will be very cooperative.

2. Some type-setting rules

Let us start with a short sample document. You can type these characters in your favorite word-processor. Nothing will happen with them, they will be interpreted once the TEX-system looks at the text.

```
\input wgndef
\title{The Title of Your Article}
{First Author, Second Author, and Third Author}
{This is the abstract of your contribution which will be printed between
two thin lines.}

\section{Introduction}%
Now you read the first sentence of the first section of the article. You
can define a new paragraph as follows:

\newpar A new paragraph starts here. Note that line breaks are formatted
by the type-setting system. Your own line breaks are not considered.
There is only one place where you should not place a line break: after a
hyphen '-' which connects two words.

\appsection{Acknowledgments}%
Sections are usually numbered. This is a section which will not get a number

\appsection{References}%
\artref{Smith A.J.}{On the Theory of Submitting Articles}
{Journal of Typesetting\/ {13 (1997)}}{pp.~55--59}
\end
```

Although this may look very weird at first glance, we have constructed a first simple, but complete article here. If you provide more text, you just fill more text in appropriate `\newpar` blocks. Note that `\newpar` is omitted after section beginnings.

Formatting of numbers and units needs some additional commands. Numbers and variables will be formatted in a maths mode which is put in `$...$`. The following example shows a Universal Time with superscript hours and minutes:

```
$22^\h53^\m$~UT
```

The tilde `~` ensures that no line break cuts the number from the UT which is not desired typographically. The date format is for instance

```
November~18, 2001
November~18-19
November~14--22
```

refers to a single night (18-19), while
refers to a *period* (14–22).

The same tilde requirement holds for all units such as

```
$125 \pm 4$~km
```

which gives 125 ± 4 km after translation by TEX. A sophisticate combination of the two is

```
$22^\h53^\m08^\s \pm 4$~s~UT
```

which could be the fairly accurate fireball timing $22^h53^m08^s \pm 4$ s UT. Some other examples show you the use of math mode for typical meteor applications:

`$m = -4$`	$m = -4$
`a magnitude $-6$ fireball`	a magnitude -6 fireball
`$V_{\rm g} = 30$~km/s`	$V_g = 30$ km/s
`$V_\infty = 32$~km/s`	$V_\infty = 32$ km/s
`${\rm ZHR} = 8.4 \pm 0.9$`	$\mathrm{ZHR} = 8.4 \pm 0.9$
`$\sol = 235\dg27 \pm 0\dg02$`	$\lambda_\odot = 235°27 \pm 0°02$

With these examples at hand, you will speed up the processing of your article considerably, since such symbols are likely to appear very often in meteor documents.

3. Figure formats

If you create image files, most of the typical formats like GIF, TIF, BMP, PCX, PNG, and JPG are fine. Note that for diagrams, the JPG format is not suitable. It is good though for photographs. All figures are converted to PostScript. If you make your graphs in PostScript anyway, send these. If you have to convert your image to PostScript, send the original image instead of the conversion result.

The figure caption should describe the graphs of photos thoroughly. Please try to avoid phrases like "refer to text". Also try to avoid multiple graphs in one figure. If you need to put them together, write a clear caption such as "Top left: Population index from meteors brighter than magnitude +2. Top right: Population index from meteors fainter than magnitude +2".

4. Tables

The editing of tables is complicated, and you need not worry about them. Use your word-processing software or the simple tabulation key to make tables. They should be unambiguous. If empfty table cells occur, it may be wise to fill them with '-'. Do not spend time on fancy formatting—the table will be reformatted completely.

5. References

The old style of references in *WGN* used numbers as citations in the text. This method is easily prone to produce errors in the order. Gradually, we will switch to citations with author plus year in *WGN*. For instance, you can write: "This was shown by Smith (1997)" or also "This was shown earlier (Smith 1997)." The style of the reference is shown in our full-article example on the previous page. The order of articles is alphabetic by first author then.

6. Author's address

At the end of each article, we publish the contact postal and e-mail addresses of the authors. Please do not forget them. You may use the following style for the addresses:

```
\appsection{Author's address}
{\it First Author\/}, Adress, City, Country, e-mail {\tt mymail@box.com}
```

and place it before the `\end` command.

7. Submission of papers

Electronic submission of articles is prefered, but printed material is also accepted (see inside back cover for addresses). You can send your paper by e-mail to `marc.gyssens@luc.ac.be` or `rarlt@aip.de`. If you send the text as an e-mail attachment, the filename should be your name (e.g. `smith.txt` or `smith.doc`). It is important to send figures separately. You can send one e-mail message, but it should contain separate attachments for the figures. The names of the figures should also include the name and the figure number (e.g. `smith_f1.gif`, `smith_f2.gif`, `smith_f3a.gif`, `smith_f3b.gif`, etc.).

8. Final remarks

Although these instructions help a lot in making the editor's life easier, we do not reject articles which have no TEX commands in it. Do not worry if you feel unsure about the formatting described. It is also fine if you insert a few of the commands or none of them. At any rate, we are looking forward to all contributions to the Journal!

June Bootid Observations in 2002

Jürgen Rendtel

In 2002, only a limited number of visual June Bootid observations is available. Weak indications for a significant rate between $\lambda_\odot = 95.4°$ and $95.7°$ are lacking confirmation. Before and after this interval rates were below the detection limit. Prospects for the 2003 and 2004 returns are shortly discussed.

1. Introduction

This shower surprised observers on 1998 June 27 with high rates lasting for several hours [1]. An earlier outbursts of comparable intensity occurred in 1916. Further possible activity enhancements were reported in 1921 and 1927. After the 1998 event the June Bootids was included in the *IMO* meteor shower working list. Not much surprising, the rates remained low in the following years as shown by Arlt [2] for the 2000 return. This is similar to the period before 1998 (data from 1995 and 1997 analyzed by Seifert [3]).

A good number of observations was reported for the interval between $\lambda_\odot = 95°$ and $98°$ of the Moon-free 2000 return. The maximum ZHR reached a level of approximately 2. The analysis of visual observations published in *WGN* [2] is based on data collected by 29 observers.

The conditions were less favorable in 2001, when a waxing Moon caused poor limiting magnitudes especially before local midnight. Furthermore, observes seem to have lost their attention after the virtual absence of the shower in 2000. Hence the number of reports was relatively small, and only very few possible June Bootid meteors were recorded. The ZHR reached a level of just 1 which makes the activity practically undetectable.

2. Observations in 2002

Nothing unusual was expected for the 2002 return, and a full Moon on June 24 caused poor conditions at most locations. We received reports from 8 observers covering the period between June 26 and early July:

> Andreas Buchmann (Switzerland), Christoph Gerber (Germany), Daniel Grün (Germany), Richard Huziak (Canada), Mike Linnolt (USA), Alastair Mcbeath (UK), Ye Quanzhi (China), Jürgen Rendtel (Germany).

The position of the 1998 maximum was reached on June 27, about 13:30 UT, hence Asian longitudes were favored. However, there is no continuous data set and the only observation from Asia was made under poor conditions (lm between +3.5 and +4.0 in the period June 27, 12:35–13:55 UT). Nevertheless, two possible shower meteors were reported. Due to the very low entry velocity of only 18 km/s, any June Bootid meteor shows a very low angular velocity, especially during the pre-midnight hours. In this period the radiant is high in the sky for nothern hemisphere observers, and meteors are thus either close to the radiant (i.e. slow moving) or near the horizon (also slow moving). Indeed, the two candidates were described being "almost as slow as satellites." It is clear that we cannot derive any significant ZHR from this data. The nearest preceeding interval covers the period June 27, 07:06–08:07 UT. The 5 shower meteors reported also indicate some activity. This period was six hours before the calculated 1998 position. Both could be interpreted like a ZHR of about 15. But a conclusion about the activity level of the June Bootids in 2002 can only be drawn if further results obtained with any technique confirm the period and the increase of rates. Further observations close to this time show nothing as can be seen in the data listed in Table 1. The last column also illustrates that the observations are just short snapshots with huge gaps between them.

3. Future returns

Recently, the outbursts of 1916 and 1998 were analyzed and modeled in detail by Asher and Emel'yanenko [4]. Particles responsible for the 1998 outburst obviously were ejected from the

parent comet 7P/Pons-Winnecke at its 1825 return. Then, a substantial portion of the meteoroids remained in a 2:1 resonance with Jupiter. A similar concentration of meteoroids was observed during the 1998 Leonids when the fireballs occurred well before the nodal passage [5] which were trapped in the 5:14 mean motion resonance with Jupiter.

Table 1 – Observational data from 2002 close to the position of the 1998 June Bootid maximum. The time lapse lists the time between the end of one observation and the begin of the following one.

Date	Period (UT)	T_{eff}	lm	JBO	Tot	Obs.	Location	time lapse
June 26	22:52–23:52	1.00	4.60	0	2	GERCH	49 N 9 E	0 h
June 26	23:20–00:22	1.00	4.98	0	2	MCBAL	55 N 2 W	6.7 h
June 27	07:06–08:07	1.00	5.1	5	7	HUZRI	52 N 107 W	4.3 h
June 27	12:35–13:55	1.33	3.8	2	2	QUAYE	23 N 113 E	7.6 h
June 27	21:30–22:45	1.20	6.40	0	15	RENJU	27 N 17 W	22.3 h
June 28	21:05–23:20	2.20	6.36	0	28	RENJU	27 N 17 W	–

Another result was obtained by Tanigawa and Hashimoto [6]. They associate the 1998 outburst with meteoroids released from the parent comet in 1819 and 1869 and perturbed into the Earth-colliding orbit by Jupiter.

Each meteoroid orbit is a modification of the parent's orbit due to ejection velocity and direction. The model calculations of Asher and Emel'yanenko [4] are consistent with an ejection velocity of 10–20 m/s for meteoroids to reach the 2:1 resonance. The discussion of particle ejection from comets using different models yielded different results over the past years, but it seems that low values of some tens of m/s are currently favored. If we assume that still a significant number of June Bootid meteoroids is in the 2:1 resonance, and that the volume containing enough particles for a good return, we could expect another June Bootid activity increase in 2004, after 0.5 orbital periods of Jupiter, with the 1998 outburst time falling on June 27, 01 UT. Trying to combine the 1921 and 1927 observations of increased June Bootid rates with the major events in 1916 and 1998, one could also suspect enhanced rates on 2003 June 27, 19 UT. Of course, the modelling indicates better chances for 2004, but the spatial extension of the meteoroid cloud is not known. The period around the possible passage deserves observations applying all techniques and participation of many observers. This is especially valid because the short northern summer nights do not allow long and overlapping intervals.

References

[1] R. Arlt, "The Analysis of a Weak Meteor Shower: The June Bootids in 2000", *WGN* 28 (2000), pp. 98–108.

[2] R. Arlt, J. Rendtel, P. Brown, V. Velkov, W.K. Hocking, J. Jones, "The 1998 Outburst and History of the June Bootid Meteor Shower", *Mon. Not. R. Astron. Soc.* 308 (1999), pp. 887–896.

[3] Seifert H., "The June Bootids in 1995 and 1997", *WGN* 26 (1998), p. 267.

[4] D.J. Asher, V.V. Emel'yanenko, "The origin of the June Bootid outburst in 1998 and determination of cometary ejection velocities", *Mon. Not. R. Astron. Soc.* 331 (2002), pp. 126–132.

[5] D.J. Asher, M.E. Bailey, V.V.Emel'yanenko, "Resonant meteoroids from Comet Tempel-Tuttle in 1333: the cause of the unexpected Leonid outburst in 1998", *Mon. Not. R. Astron. Soc.* 304 (1999), pp. L53–L56.

[6] T. Tanigawa, T. Hashimoto, "The origin of the 1998 June Bootid meteor shower", *Earth, Moon, and Planets* 88 (2000), pp. 27–33.

Author's address

Jürgen Rendtel, Seestr. 6, D-14476 Marquardt, Germany, e-mail `jrendtel@aip.de`.

Meteor Orbit and Trajectory Software (MOTS)—Determining the Position of a Meteor with Respect to the Earth Using Data Collected with the Software MetRec

D. Koschny and J. Diaz del Rio, ESA/ESTEC

We describe a new software called "Meteor Orbit and Trajectory Software" (MOTS) which determines trajectory information of a meteor using data obtained with the software MetRec. The algorithm used in the software is explained, as well as the information in the output files.

1. Introduction

This paper derives a robust way of determining the altitude of meteors. The algorithm is implemented in a software tool called MOTS (Meteor Orbit and Trajectory Software utility). MOTS reads input from double-station observations analyzed with the software MetRec.

MetRec is an automated meteor detection software written by Sirko Molau [1]. A Matrox Meteor frame-grabber card digitizes video meteor data. The digitized images are examined by the software for meteors. For each meteor, an overall entry in a log file is written, giving the appearance time of the meteor, and its position in relative coordinates. The program 'RefStars', also written by Sirko Molau, reads in one image recorded by the camera, the time of the image, and the position of the camera. It then allows to compare the stars on the image with a star catalog and thus allows to determine the pointing position of the camera. If this was done, MetRec uses the information to assign the coordinates in right ascension and declination to each meteor. It also uses the magnitude information of the stars to estimate the magnitude of the meteor (albeit this is still very inaccurate in the current version of MetRec and cannot really be used for scientific purposes).

Optionally, MetRec can write a detailed information file (`*.inf` file) for each meteor. It lists for each frame when the meteor is visible the exact time (in steps of 0.04 s), with it the magnitude estimate and the position of the meteor.

If double-station observations of the same meteor are available, the precise trajectory in space of this meteor can be determined. This is the task of our new software, Meteor Orbit and Trajectory Software (MOTS): It reads in the `*.inf` files of one meteor seen from two different stations. It also needs to know the position of the two observing stations. From this information, it calculates the following:

1. The trajectory of the meteor with respect to the Earth. In particular, it determines for each individual image of the meteor as recorded by one station the altitude above the Earth in km and the distance to the observer. This information is important to e.g. analyze meteor spectra, where it is interesting to know at which altitude a meteor was when a certain spectral line became active. The distance to the observer is needed to correct the observed apparent magnitude to absolute magnitude (the magnitude of the meteor as seen from 100 km distance).
2. The radiant of the meteor, i.e. the direction where the meteor came from, and from that the orbit of the meteor around the Sun. This information is relevant to study trajectories of the meteoroids or to draw conclusions on the ejection process on the parent comet.

A detailed description for MOTS is available in [2]. Short user and installation manuals will be available on the *IMO* web site where the code can be downloaded. This paper concentrates

on describing the algorithm on how the calculations were done. For the sake of precise documentation of the code, we define in this paper the routines as they are implemented in the C code of the program and go down to the basics of analytical geometry. The mathematically not so experienced reader may read the appendix first to get a refresh of the basics of vectors and vector analysis.

2. Finding the position of the meteor with respect to the Earth—overview

The precise position of the meteor can be determined if we have observations from two different stations, henceforth called 'station 1' and 'station 2', located some distance apart. To result in a good geometry, station 1 and 2 should be between 60 and 100 km apart. We assume that each station uses a video camera that will give us the position of a meteor in right ascension and declination for a number of individual video frames. The information that we need to determine the precise path of the meteor is:

1. The position of the two stations on the Earth, i.e. their latitude, longitude, and elevation.
2. The viewing direction towards the meteor from the two stations, i.e. right ascension (RA) and declination (Dec) from station 1 and station 2. When using video cameras, we will have one value of RA and Dec for each video image.
3. The time and date of the observation.

The position of the two stations can be read from a map or determined with a GPS receiver. The viewing directions RA and Dec will be determined either automatically, e.g. by the software MetRec, or measured manually. MOTS assumes that the information is available in the form of `*.inf`-files as generated by MetRec.

The time of the observation is, of course, identical for the two stations. If e.g. the computer clock or a time inserter is used for the video signal, the recorded time might be off by several seconds during the course of a night, unless it is constantly synchronized. This has to be taken into account in the algorithm.

One possibility to determine the altitude of a meteor is to determine the direction of the meteor at one precise point in time as seen from one station, then look at the direction as seen from the other station. Without any measurement errors, the two lines should intersect. In practise, they will be off a little bit due to measurement errors. Finding the shortest distance between the two lines and assuming that the meteor lies halfway in between should yield the position of the meteor. Albeit, since the precise timing of individual video frames may not be known, this method can yield results that are extremely wrong. We therefore choose a different approach.

First only consider the algorithm that takes this information and determines the altitude of the meteor. Consider Figure 1 for a graphical representation.

To determine the altitude of the individual meteor positions as determined by station 1, we first find the plane that is defined by the meteor observations from station 2 and station 2 itself. Using the viewing direction of two points of the meteor as two vector directions does this. The cross product of these two vectors defines the normal of the plane, with station 2 being part of the plane. We go through all possible combinations of vectors (first frame containing the meteor with the second, first and third, first and fourth, ..., second and third, second and fourth, and so on) and find the average normal vector. This, together with the point of station 2, defines the plane. Since the error will be larger for points that are close together, we use weights for the average that are proportional to the angle between the vectors.

Now consider station 1 and the viewing direction to define the line of sight of the meteor in frame i as seen from station 1. Using vector analysis, we find the intersection between the plane and the line in earth-centered $x/y/z$ coordinates. Subtracting the Earth's radius yields the altitude above the surface.

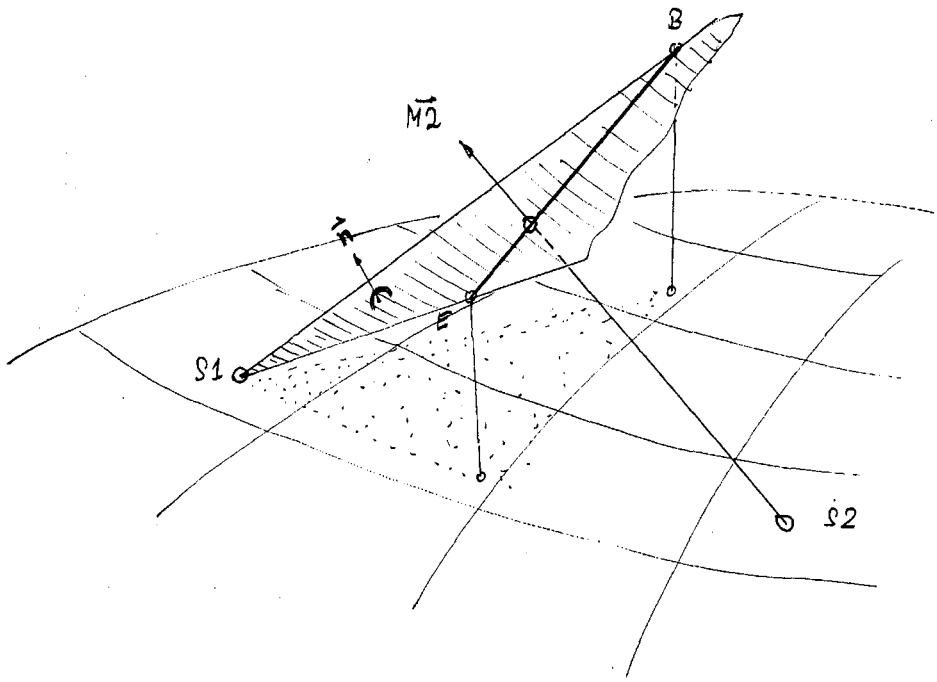

Figure 1 – Geometry of a meteor as seen from two stations. S_1, S_2: Station 1, 2. A meteor flies from point A to B. n is the normal vector of the plane, M_2 the viewing direction to one point of the meteor as seen from S_2.

Applying the method of linear fitting of n-dimensional points using orthogonal regression, a line is fitted to the set of points in three-dimensional space. Each measured point of the meteor is projected onto this line. The velocity versus time is determined by dividing the distance between two consecutive points and the time interval. The average velocity is found by using the distance between the first and the last point of the meteor. To get an idea of the error of the velocity determination, the standard deviation of the average of all individual velocity determinations is calculated.

The backward direction of the line is computed in right ascension and declination and gives the apparent radiant of the meteor.

MOTS will scan two different directories which contain `*.inf` files of double-station meteors. It uses the log-files to find the meteors that were observed. It takes the ref-files to get the latitude and longitude of the two stations. It then looks at the `*.inf`-files to retrieve the detailed positional information of a double-station meteor. From this information, it will calculate the altitude of a meteor for each frame listed in the `*.inf`-file, and the velocity. It will generate one file per meteor, listing this information as seen from each station, called `*.daf` (detailed altitude file). It will generate one summary file per directory that lists all double-station meteors with their average velocity, the radiant they appear to come from, and begin and end height. For each value, error estimates are given.

A future step of this software is to convert the geocentric position of the meteor to a heliocentric and to determine the orbit of the particle producing the meteor. That, however, is beyond the scope of this article.

3. Some convenient routines

3.1. Coordinate systems and naming conventions

To perform the necessary calculations, we need to define a convenient orthogonal coordinate system, which allows us to write down all the positions in vector notation. When performing the calculations with respect to the Earth, we will use a coordinate system as shown in Figure 2.

The x-axis is in the equatorial plane of the Earth, pointing towards vernal equinox. The z-axis is going through the center of the Earth and the North Pole. The y-axis completes the right-handed coordinate system.

This coordinate system will be referenced hereafter as 'XYZ'.

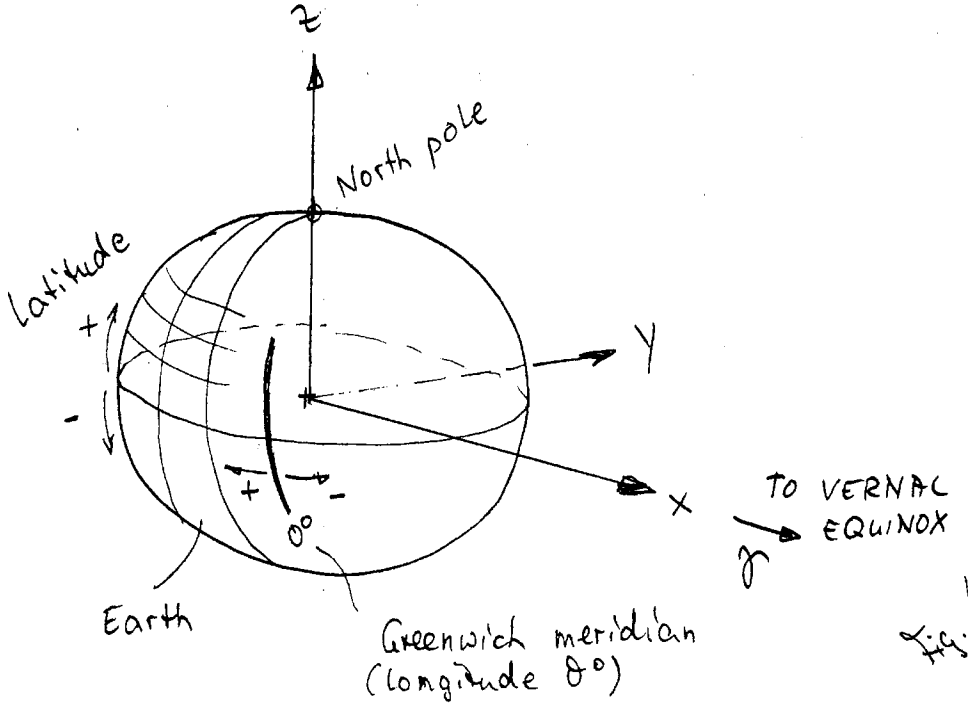

Figure 2 – Earth-centered orthogonal coordinate system.

Additionally, we will use the standard coordinate system used to describe positions on the Earth, namely latitude (the distance to the equator—the North Pole is at $+90°$, the South Pole at $-90°$. The longitude is measured with respect to the zero meridian defined as going through Greenwich. The elevation or altitude is the height above mean zero in meter or kilometer. To obtain mean zero, we will later approximate the Earth by a rotational ellipsoid.

This coordinate system will be abbreviated 'GEO'.

The celestial coordinate system uses right ascension and declination, similar to latitude and longitude on the Earth. The celestial equator is where the extension of the Earth's equator crosses the imaginary stellar sphere. The right ascension corresponds to the longitude on the Earth. The zero point is defined where the ecliptic crosses the celestial equator, the vernal equinox. The distance to the celestial equator is the declination, with $+90°$ the celestial North Pole. We will abbreviate this coordinate system with 'Cel'.

3.2. The radius of the Earth as a function of latitude (r_{earth})

In the routines used here, we approximate the Earth with a rotational ellipsoid as shown in Figure 3. The equatorial radius is $a = 6378388$ m, the polar radius is $b = 6456911.9$ m.

To find the radius r at latitude ϕ we start with the equation for an ellipse:

$$\frac{x^2}{a^2} + \frac{y^2}{b^2} = 1$$

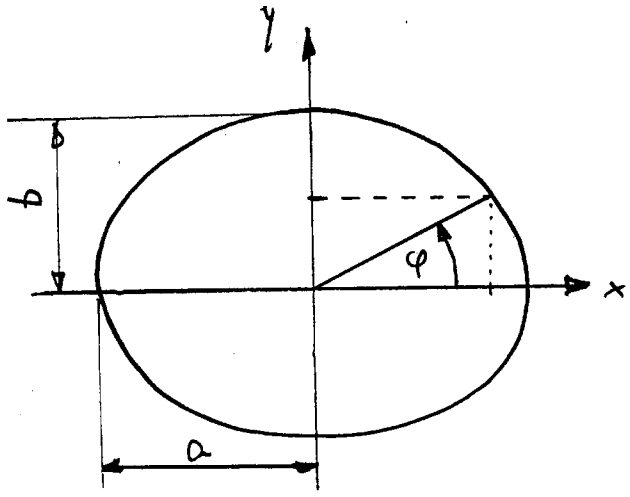

Figure 3 – Cross-section through the Earth, approximated by a rotational ellipsoid.

From basic geometry, we know

$$r = \sqrt{x^2 + y^2}$$

$$\frac{y}{x} = \tan\phi$$

Solving the equation of the ellipse (1), for y and equating with (3) results in

$$y = \sqrt{b^2 - \frac{b^2}{a^2}x^2}$$

$$\frac{y}{x} = \sqrt{\frac{b^2}{x^2} - \frac{b^2}{a^2}} = \tan\phi$$

From (2) we get

$$r^2 = x^2 + y^2 = x^2 + b^2 - \frac{b^2}{a^2}x^2 = x^2\left(1 - \frac{b^2}{a^2}\right) + b^2$$

Solving (4) for x^2 gives

$$(\tan\phi)^2 = \frac{b^2}{x^2} - \frac{b^2}{a^2};$$

Rearranging:

$$x^2 = \frac{a^2}{\left(\frac{a}{b}\tan\phi\right)^2 + 1}$$

Substituting in (5) yields the final value for the radius r as a function of the latitude ϕ:

$$r = \sqrt{\frac{a^2 - b^2}{\left(\frac{a}{b}\tan\phi\right)^2 + 1} + b^2}$$

3.3. Julian Date (JD)

The Julian Date is commonly used to describe dates and times in astronomy. It is based on the Julian calendar and counts the days starting from January 1, 4713 B.C. The beginning of the day is 12^h UTC. In all our calculations, we use the Julian Date, since it is monotonously increasing. Formulae to convert normal calendar dates to JD and vice versa can be found in any astronomical formula book.

3.4. Local Mean Sidereal Time (LMST)

The Local Mean Sidereal Time is the right ascension that is at the meridian (the North-South line) for a given time as seen from a certain longitude on the Earth. In other words: it is the angle between the current longitude and the direction to vernal equinox, see Figure 4.

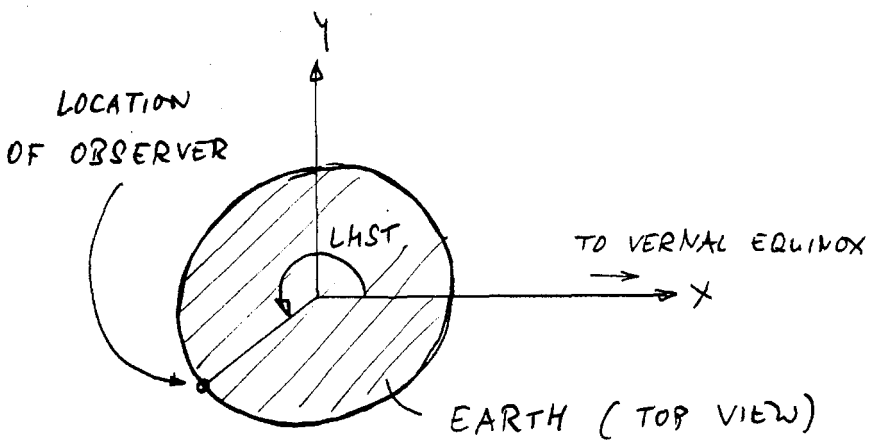

Figure 4 – Illustration of the Local Sidereal Mean Time. The circle is the Earth as seen from the direction of the North pole, the $+x$ axis points to the direction of vernal equinox.

From astronomical textbooks we get the formula to convert the date and time in Julian Date to LMST:

$$\text{LMST} = 6.656306\ \text{h} + 0.0657098242\ \text{h}(\text{JD} - 2445700.5) + 1.0027379093\,t + \Lambda/15^\circ$$

Where JD is the Julian Date, t the time in decimal hours UTC, Λ the longitude of the observing site.

3.5. Converting geographical coordinates to $x/y/z$ coordinates (Geo2XYZ)

The geographical coordinates are longitude Λ, latitude ϕ, and elevation h. To convert them to $x/y/z$ coordinates the standard conversion between spherical and orthogonal coordinates is used:

$$x = (r\,(\phi) + h) \cdot \cos(\phi) \cdot \cos(\text{LMST})$$
$$y = (r\,(\phi) + h) \cdot \cos(\phi) \cdot \sin(\text{LMST})$$
$$z = (r\,(\phi) + h) \cdot \sin(\phi)$$

where $r(\phi)$ is the radius of the Earth as determined by (7). We will henceforth refer to this function as $\vec{p} = \text{Geo2XYZ}\,(\Lambda, \phi, h, t)$ where $\vec{p} = (p_x, p_y, p_z)$ a vector in Earth-centered orthogonal coordinates.

3.6. Converting $x/y/z$ coordinates to geographical coordinates (XYZ2Geo)

This routine is the inverse of the above. It converts a point $\vec{p} = (p_x, p_y, p_z)$ to latitude, longitude, and an altitude above mean sea level, taking into account the Earth's oblateness by using equation (7) to determine the Earth's radius as a function of latitude. A time needs to be passed to this function to know the rotational position of the Earth.

3.7. Converting right ascension and declination to a vector (Cel2XYZ)

The right ascension and declination are the coordinates of a point at the celestial sphere. This imaginary sphere can be considered to be in infinite distance. This means that right ascension and declination can be converted to a direction of a vector in our orthogonal coordinate system

only, the length is not known. Again we use the standard conversion between spherical and orthogonal coordinates. The radius r is set to $r = 1$ in this case and we get

$$x = \cos(\text{Dec}) \cdot \cos(\text{RA})$$

$$y = \cos(\text{Dec}) \cdot \sin(\text{RA})$$

$$z = \sin(\text{Dec})$$

We will refer to this function as Cel2XYZ(RA, Dec) where RA the right ascension, Dec the declination.

3.8. Converting directions in $x/y/z$ coordinates to right ascension and declination (XYZ2Cel)

This routine is the inverse of the above. It is needed e.g. to convert the flight direction of the meteor towards its radiant.

4. The detailed analysis process

4.1. Determination of the stations in $x/y/z$ coordinates

All our calculations are done in an orthogonal, Earth-centered coordinate system. So the first step is to convert the position of station 1 and station 2 to $x/y/z$ coordinates. This can easily be done using the routine Geo2XYZ described in Section 3.5. For both stations, longitude, latitude, and altitude are known. The middle time of the meteor as seen from station 1 is used to determine the coordinates for station 1, the middle time of the meteor as seen from station 2 is used for station 2.

$$\vec{S_1} = \text{Geo2XYZ}(\Lambda_1, \phi_1, h_1, t_1)$$

$$\vec{S_2} = \text{Geo2XYZ}(\Lambda_2, \phi_2, h_2, t_2)$$

where $\vec{S_1}$ is the vector from the center of the Earth to station 1, respectively, ibid. for station 2. Λ_1, ϕ_1, h_1, are the longitude, latitude, and altitude for station 1, ibid. for station 2. t_1 and t_2 are the medium time for the meteor as seen from the respective station.

4.2. Determination of the viewing directions

The viewing direction of each individual video image is given by the right ascension and declination of the meteor as seen in the respective image. It is the direction of the vector from the station towards the meteor. This direction can be calculated by using the routine Cel2XYZ. It will give a vector with unit length, as the distance to the meteor is not yet known.

Let us call the directional vector to the meteor as seen from station 1 $\vec{M}_{1,i}$, with i the number of the meteor frame, starting from 0. The corresponding vector as seen from station 2 will be $\vec{M}_{2,j}$ with j the number of the meteor frame, starting from 0.

$$\vec{M}_{1,i} = \text{Cel2XYZ}(\text{RA}_{1,i}, \text{Dec}_{1,i})$$

$$\vec{M}_{2,j} = \text{Cel2XYZ}(\text{RA}_{2,j}, \text{Dec}_{2,j})$$

4.3. Find the plane through station 2

A plane is defined as

$$(\vec{a} - \vec{x}) \cdot \vec{n} = 0$$

where $\vec{a}$ one point of the plane and $\vec{n}$ is the normal vector to the plane. In this case, $\vec{a}$ is the vector to station 2, i.e. $\vec{S_2}$ as determined by (10). The normal vector can be found by taking the cross product of any two vectors from station 2 to the meteor:

$$\vec{n}_{l,m} = \vec{M}_{2,l} \times \vec{M}_{2,m}$$

The number of viewing directions corresponds to the number of video images in which the meteor is visible. We determine the normal vector from going through all permutations of two vectors and average the result. Since the uncertainty in the calculation gets larger for smaller angles between the two vectors, we apply a weighing factor when taking the average. This factor is proportional to the angle between the two vectors—the smaller the angle, the smaller the weight and thus the contribution to this vector combination to the average. The average vector is called $\vec{n}_{2,av}$.

4.4. Finding the intersection between the plane through station 2 and each viewing direction from station 1

Now we have both $\vec{a}$ and $\vec{n}$ defined in (12). We can find the position of the meteor in the Earth-centered coordinate system by looking at the viewing directions (i.e. the right ascension and declination) of the meteor in each video image as seen from the other station, station 1, $\vec{M}_{1,i}$ as determined from (11). The intersection between this vector and the plane will give us the position of the meteor for that video image. The line l of the viewing direction can be described by

$$l: \quad \vec{x} = \vec{S}_1 + \lambda \vec{M}_{1,i}$$

Using (12), we can write the plane through station 2 as

$$P: \quad \left(\vec{S}_2 - \vec{x}\right) \cdot \vec{n}_{2,av}$$

Plugging (14) in (15) and solving for λ, we get

$$\lambda = \frac{\vec{S}_1 \cdot \vec{n}_{av} - \vec{S}_2 \cdot \vec{n}_{av}}{\vec{M}_{1,i}\vec{n}_{av}}$$

We put (16) back into (14) and get the $x/y/z$ coordinates in meters for the point of the meteor as seen in video image i from station 1 as

$$\vec{x}_{1,i} = \vec{S}_1 + \frac{\vec{S}_1 \cdot \vec{n}_{av} - \vec{S}_2 \cdot \vec{n}_{av}}{\vec{M}_{1,i}\vec{n}_{av}} \vec{M}_{1,i}$$

This calculation is done for each video image containing the meteor. The result will be a set of $x/y/z$ coordinates for the meteor.

4.5. Determining sub-point and altitude for each point of the meteor

Here we use the routine XYZ2Geo to convert the vector obtained in (17), together with the time recorded for the respective video image, to latitude, longitude, and elevation. The latitude and longitude are the coordinates on the Earth's surface under the meteor point. The elevation is its distance above mean sea level. This information will be written in the Detailed Altitude File (`*.daf`). There will be one entry per video image in such a file.

4.6. Finding the distance to the camera

The absolute value of the vector difference between the $x/y/z$ coordinates of the meteor and the location of the station is the distance between camera and the meteor:

$$d_{1,i} = |\vec{M}_{1,i} - \vec{S}_1|$$

This value will also be written to the Detailed Altitude File for each video image. This number is important e.g. to convert the apparent magnitude of the meteor in that point to the absolute magnitude (defined as the magnitude as seen from 100 km distance).

4.7. The best fit line to the meteor's path and determining the velocity

The method of linear fitting of n-dimensional points using orthogonal regression is used to find the best fit line to all data points obtained from the observations of station 1. See [3] for a detailed description on this method.

The measured $x/y/z$ points will scatter around the best fit line. We project them onto the best fit line, again using standard analytical geometry routines. These points are then used to calculate a velocity associated to each point. This value is documented in the Detailed Altitude File (`*.daf`). For an illustration, see Figure 5.

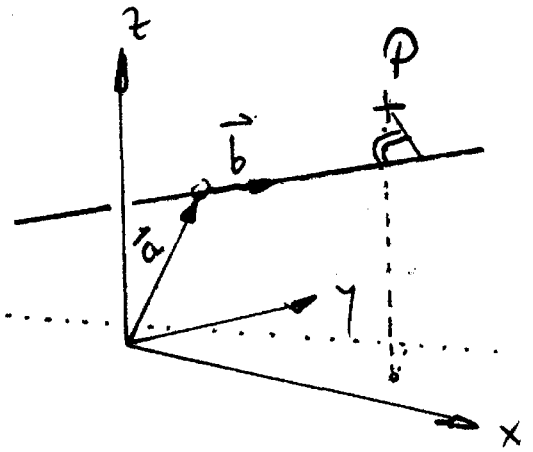

Figure 5 – Projection of a point onto a line.

Each individual velocity is a vector. Its backward direction is converted to right ascension and declination. The standard deviation of all of these values is used as an error estimate for the radiant of the meteor. The standard deviation of the average of the absolute values of the velocities is used as an estimate of the average velocity. Note that the average velocity is not determined from the individual values, rather the first and the last observed point of the meteor trajectory and their time difference are used. Tests showed that this method actually is more accurate than taking the average of all individual values.

The backward direction of the best fit line (i.e. opposite the flight direction of the meteor) is converted to celestial coordinates using the routine XYZ2Cel. The obtained right ascension and declination are the radiant of the meteor, as seen from station 1. This value is written into the Orbit File (`*.orb`), together with the error estimate determined from the individual velocity vectors for each video image.

4.8. The other observing station

As a result of the above, we obtain one `*.daf` file for one station giving details for each individual video image of a meteor, plus one line in the `*.orb` file for a complete directory, i.e. one complete observing night. Now we reverse the role of station 1 and station 2. This means, we find the plane determined by station 1 and the meteor as seen from station 1, and look at each individual video image of the meteor as seen from station 2. Again, we will find $x/y/z$ coordinates, a best fit line, velocities versus video image, and a radiant. A separate `*.daf` file and a second line in the `*.orb` file is created. The deviation between the observations from station 1 and station 2 will give an idea about the overall errors that the measurement has.

5. Final output

In summary, we obtain two different types of output. For each meteor and each observing station, we obtain a "Detailed Altitude File", with the filename hhmmss.daf, where hhmmss is the hour, minute, second of the time of the meteor. The format of this file follows the format of the `*.inf`

files of MetRec. It contains a header giving information about filenames and pathnames and the appearance time of the meteor accurate to one second (identical to the file name). Then there is one line for each observed video image that gives the following information:

- A consecutive number.
- The time of the video image in decimal seconds.
- The apparent brightness of the meteor in stellar magnitudes.
- The relative x and y position of the meteor in the field of view.
- The calculated altitude of the meteor in meters with an error estimate.
- Latitude and longitude of the point under the meteor.
- Distance to the camera in meters with an error estimate.
- The velocity as calculated between this video image and the previous one, plus an error estimate.

This information is repeated twice—once for the meteor as seen from station 1, once as seen from station 2.

For each directory, i.e. for each complete night of an observation, there will be an Orbit file with the name `yyyymmdd.orb`. `yyyy` is the year, `mm` the month, and `dd` the day of the observation. This file will have two lines per meteor, the first line based on the data as observed by station 1, every second line based on the data as observed by station 2. Again, there is a header giving information about the directories and filenames. It repeats the configuration parameters that were set to run the program. Then there are two lines for each meteor listing the information as determined by the two stations:

- Consecutive number of meteor
- Number of station
- Time of the meteor, accurate to one second (corresponds to the name of the `*.daf` file)
- Begin and end position in relative coordinates in the video image. This allows to assess whether the full path of the meteor was visible in the image.
- Maximum apparent magnitude and absolute magnitude (the magnitude of the meteor as seen from 100 km distance).
- Average velocity and an error estimate in km/s.
- Begin and end height of the meteor with an error estimate in km/s.
- Right ascension and declination of the radiant, together with and error estimate for both coordinates.

In the future, we will add the orbital elements of the meteor. This, however, will be the subject of a separate paper. The software will be available from the IMO ftp server (`ftp.imo.net`), navigate to 'MOTS'. The distribution includes an executable of the code, sample files, and a user guide.

6. Encountered problems

One of the difficulties that were encountered in the testing of the software is the fact that the time inserters of the two cameras observing the same area in the sky are not perfectly synchronized. We performed tests with data obtained in the ESA Leonid campaign 2002 from Australia. We used the time inserter produced by Prof. Cuno, Germany, to insert the time into the video signal. The time inserters were synchronized via a GPS receiver (Garmin etrex) at the beginning of the night. After that, the internal clocks of the inserters were left running without synchronization. Apparently, the clocks drift, and they drift in different directions and not linearly. Allowing a time window for the identification of simultaneous meteors of a few seconds was necessary. Then of course the question arises as to which time to use for the calculations. We decided to use the average time of the two observations for the calculation of the plane. This will introduce an error: Assume the error to be 1 second. In that time, a point at the Earth's equator would would move just because of the rotation of the Earth by about 460 m. Fortunately, it will only result in a tilt of the plane, so the real error introduced into the altitude of the meteor will be smaller. The detailed value depends on the precise geometry.

As a conclusion, we recommend to continuously synchronize the clocks via GPS or (in Europe) via the DCF77 signal.

First test runs were done with data obtained during the ESA/RSSD Leonid campaign from Australia [4]. There, we recorded double-station meteors on video tape for four nights around the Leonid peak. The tapes were later analyzed by MetRec. There we found a second point of concern: the estimated error in the radiant position was typically about 0°.1, all observed meteor points lay very close to the best fit line of the meteor's path (less than 50 m). However, the error in velocity sometimes was as large as 10 km/s. Looking at the Detailed Altitude Files, we realized that MetRec sometimes did not record the center of a meteor track in one frame, but the recorded position was offset in the direction of the flight path. One of the reasons for this could be that some meteors develop a small wake behind the head which then is taken into account into the determination of the photometric center of the meteor.

This can be avoided by visually analyzing the measured meteor positions and fine-tuning them via a manual process.

References

[1] Molau, S. and Nitschke, M., "Computer-based Meteor Search", *WGN* 24, 1996, pp. 119–123.

[2] Diaz del Rio, J., "Meteor Orbit and Trajectory determination Software (MOTS) and MetGrab, two tools for meteor analysis", Stagiaire Report ESA/RSSD, 2002.

[3] "Least Squares Linear Fitting", `http://www.magic-software.com/Doc.html`.

[4] Koschny, D., Trautner, R., Zender, J., Knöfel, A., Witasse, O., "The ESA Leonids 2001 Expedition to Australia", Asteroid, Comets, Meteors, 29 July–2 Aug, 2002, Berlin (poster).

Appendix—vectors and describing lines and planes

Introduction

In this section, we repeat some basic definitions of vectors and vector analysis. The reader who is familiar with these mathematical procedures is kindly asked to skip it.

What's a vector

Let's assume that we use a right-handed geocentric coordinate system, i.e. a system with three perpendicular axes x, y, z (see Figure 2). Three coordinates can now describe any point in space. A vector is the line from the origin of the coordinate system to this point and will be written as

$$\vec{a} = \begin{pmatrix} a_x \\ a_y \\ a_z \end{pmatrix}$$

Vectors can be added and subtracted by adding and subtracting their components:

$$\vec{c} = \vec{a} + \vec{b} = \begin{pmatrix} a_x + b_x \\ a_y + b_y \\ a_z + b_z \end{pmatrix}$$

The length of a vector, or its "absolute value," can be calculated by

$$|\vec{a}| = \sqrt{a_x^2 + a_y^2 + a_z^2}$$

Describing a line using analytical geometry

A line g in three-dimensional space can be described by one point on the line and a directional vector. To find any point on the line, the directional vector is multiplied by a scalar factor, the value of which is left open:

$$g: \quad \vec{x} = \vec{p} + \lambda\vec{q}$$

Figure 6 illustrates this.

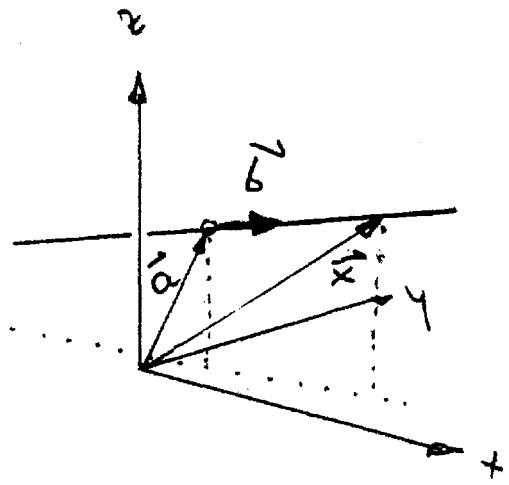

Figure 6 – Describing a line using analytical geometry.

The scalar product

The scalar product of two vectors results in a scalar number. If φ is the angle between two vectors, the scalar product is defined as

$$\vec{a} \cdot \vec{b} = |\vec{a}| \cdot |\vec{b}| \cdot \cos\varphi$$

with φ between 0° and 180°. The scalar product really gives the projection of vector $\vec{a}$ projected on $\vec{b}$, multiplied with $\vec{b}$, or the vector $\vec{b}$, projected on $\vec{a}$ and multiplied with $\vec{a}$.

The cross product

The cross product of two vectors results in another vector. The absolute value of the result is the volume of the parallelogram described by the two vectors. If j is the angle between two vectors, the cross product is defined as

$$\vec{c} = \vec{a} \times \vec{b}$$

$$|\vec{c}| = |\vec{a}| \cdot |\vec{b}| \cdot |\sin\varphi|$$

Describing a plane using analytical geometry

To describe a plane, we use the normal vector $\vec{n}$ of the plane and one point $\vec{a}$ that the plane contains. The difference between any point $\vec{x}$ in the plane and $\vec{a}$ will be perpendicular to the normal vector. Remembering that the scalar product of two vectors that are perpendicular is zero, we can write for the plane E:

$$E: \quad (\vec{a} - \vec{x}) \cdot \vec{n} = 0$$

Figure 7 illustrates this.

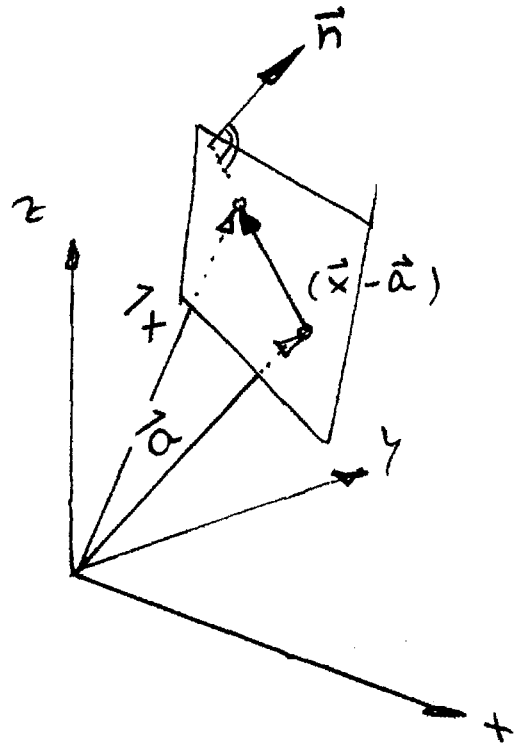

Figure 7 – Describing a plane using analytical geometry.

The intersection between a plane and a line

To find the intersection between a plane and a line, we take the equation for the plane and replace $\vec{x}$ with the equation for the line:

$$(\vec{a} - (\vec{p} + \lambda\vec{q})) \cdot \vec{n} = 0$$

This can be rewritten to

$$\vec{a}\vec{n} - \vec{p}\vec{n} + \lambda\vec{q}\vec{n} = 0$$

$$\lambda = \frac{\vec{p}\vec{n} - \vec{a}\vec{n}}{\vec{q}\vec{n}}$$

With this equation we can determine the scalar λ that, plugged back into the equation for the line, will give us the value for the intersection point.

The projection of a point on a line

Assume a point $\vec{m}$ close to a line described by $g: \ \vec{x} = \vec{p} + \lambda\vec{q}$. We want to find the projection of the point onto the line, i.e. find the normal vector to the line that goes through the point $\vec{m}$ and its location on the line. Two boundary conditions constrain the normal vector: One point has to lie on the line g, therefore there must be a value λ_0 such that

$$\vec{m}_0 = \vec{p} + \lambda_0\vec{q}$$

The normal vector is perpendicular on g, i.e.

$$(\vec{m}_0 - \vec{p}) \cdot \vec{q} = 0 \quad \text{or} \quad \vec{m}_0\vec{q} = \vec{p}\vec{q}$$

Now we can write the projected point $\vec{m}_0$ as

$$\vec{m}_0 = \vec{p} + \frac{(\vec{m} - \vec{p}) \cdot \vec{q}}{\vec{q}^{\,2}} \cdot \vec{q}$$

The distance between the point and its projection can be written as

$$d = \frac{|\vec{q} \times (\vec{m} - \vec{p})|}{|\vec{q}|}.$$

7. Appendix: Sample orbit files

```
Station1Directory: 'C:\METREC3.5\DATA\ICC2\20011118\'
Station2Directory: 'C:\METREC3.5\DATA\LCC3\20011118\'
MaxDeltaTime: 3.00 sec
MaxMeaningfulAltitude: 180.0 Km
MinMeaningfulAltitude:  40.0 Km
TimeOffSet: 00:00:00.00
ParallelLogFiles: 1

!-------------------------------------------------------------------------------
LogFile:                '20011118.LOG'
RefStarFilenameStation1: 'C:\METREC3.5\DATA\ICC2\20011118\20011118.ref'
RefStarFilenameStation2: 'C:\METREC3.5\DATA\LCC3\20011118\20011118.ref'
AppearanceDate: 2001/11/18
!-------------------------------------------------------------------------------

!                    Pos. (begin)    Pos. (End)   Max.  Max Obs  Velocity (Km/s)      Height (meters)          Radiant (RA:Dec Hours, Dec:°)  Orbital Elements
!### Station   Time        x       y       x       y    Mag.    Mag.      v      ±v      Begin      End    ±pos    alpha    ±a     delta    ±d   Parameters of orbit
001       1  17:25:27  0.721   0.022   0.762   0.122   3.9     4.4     58.571  1.221   126189.5   125299.7   1.5   10.215  0.000  21.456  0.000
001       2  17:25:26  0.551   0.592   0.361   0.944   1.6     2.0     71.066  2.080   121980.6   115942.2  35.7   10.253  0.000  21.548  0.000
002       1  17:31:21  0.046   0.621   0.122   0.960   4.5     4.9     71.484  1.923   123387.5   120310.1   5.8   10.208  0.000  20.859  0.000
002       2  17:31:20  0.413   0.215   0.232   0.478   1.9     2.2     70.726  2.646   120658.0   114841.8  28.6   10.238  0.000  21.096  0.000
003       1  17:37:34  0.686   0.014   0.983   0.819   5.9     6.2     68.651  21.147  122070.9   114720.2  20.4   10.255  0.000  21.334  0.000
003       2  17:37:33  0.677   0.382   0.368   0.961   2.5     2.7     71.052  6.474   122896.3   110033.8  65.1   10.287  0.000  21.423  0.000
004       1  17:43:27  0.534   0.579   0.643   0.968   7.0     7.4     63.858  10.405  121830.0   118001.3   6.6   10.233  0.000  21.110  0.000
004       2  17:43:26  0.487   0.463   0.280   0.809   2.1     2.3     71.023  2.257   119528.3   111382.4  30.1   10.266  0.000  21.273  0.000
005       1  17:43:46  0.010   0.514   0.030   0.638   4.2     4.4     62.781  11.599  108747.2   107386.7  42.5   10.178  0.000  21.122  0.000
005       2  17:43:45  0.663   0.017   0.443   0.351   1.4     1.5     70.527  2.469   115058.9   104114.4  25.9   10.198  0.000  21.315  0.000
006       1  17:45:43  0.246   0.585   0.284   0.775   4.1     4.7     72.983  13.468  130805.8   128421.3  72.4   10.186  0.000  20.815  0.000
006       2  17:45:42  0.327   0.414   0.154   0.666   1.4     1.8     71.166  1.062   122728.5   116066.4  33.1   10.209  0.000  21.034  0.000
007       1  17:46:20  0.127   0.591   0.195   0.973   5.1     5.5     65.825  25.717  119852.9   115491.6  55.0   10.192  0.000  20.852  0.000
007       2  17:46:19  0.530   0.147   0.174   0.673   1.5     1.9     71.051  1.702   121018.0   106286.7  83.2   10.223  0.000  21.104  0.000
008       1  17:51:57  0.260   0.131   0.382   0.690   4.7     4.9     68.489  17.580  118733.3   111697.4  15.2   10.226  0.000  20.793  0.000
008       2  17:51:56  0.553   0.341   0.511   0.411   2.2     2.5     68.700  0.399   113853.0   111548.7  22.8   10.255  0.000  20.961  0.000
009       1  17:55:22  0.189   0.260   0.321   0.979   4.2     4.8     68.642  21.353  131184.6   121581.8  82.3   10.250  0.000  21.147  0.000
009       2  17:55:21  0.571   0.101   0.161   0.698   1.9     2.5     68.536  11.585  130905.1   111149.4  90.5   10.285  0.000  21.417  0.000
```

Figure 8 – Sample orbit files (excerpt of 20011118.orb for ESA's ICC2)

8. Appendix: Sample detailed altitude file

```
Station 1
LogFile:            '20011118.LOG'
StationDirectory: 'C:\METREC3.5\DATA2\ICC2\'
AppearanceDate: 2001/11/18
AppearanceTime: 18:36:34
RefStarFilename: 'C:\METREC3.5\DATA2\ICC2\20011118\20011118.ref'
INFFilename: 'C:\METREC3.5\DATA2\ICC2\20011118\183634.INF'
FrameCount: 19

!                           Position          Altitude (m)          SubPoint        Dis. to Camera (m)  Velocity (Km/s)
!###   Time  Bright      x      y         h       ±h    ±pos    lon (°)   lat (°)    Dis. Cam.   ±D2C       v       ±v
 001  34.62    5.5   0.389  0.039  140736.5   35.0   40.9   123.668  -17.705   179263.1   15.0    -------  ------
 002  34.66    4.5   0.391  0.078  139636.2   31.6   36.9   123.650  -17.717   177098.1   13.7     63.647   5.165
 003  34.70    4.5   0.393  0.120  138489.9   27.1   31.6   123.632  -17.729   174851.4   11.9     66.411   2.401
 004  34.74    3.4   0.396  0.175  137002.1   25.5   29.7   123.608  -17.744   171960.2   11.4     86.029  17.216
 005  34.78    3.5   0.399  0.216  136000.2   22.9   26.7   123.591  -17.755   169950.5   10.4     60.726   8.086
 006  34.82    3.1   0.401  0.266  134723.4   20.2   23.6   123.570  -17.769   167500.4    9.3     73.712   4.900
 007  34.86    2.6   0.404  0.315  133497.0   20.9   24.4   123.551  -17.781   165155.6    9.7     71.053   2.240
 008  34.90    2.7   0.407  0.372  132133.5   33.1   38.7   123.529  -17.796   162550.5   15.7     79.732  10.920
 009  34.94    2.5   0.409  0.424  130898.2   23.7   27.6   123.509  -17.809   160234.7   11.4     71.113   2.301
 010  34.98    1.2   0.411  0.476  129645.0   19.8   23.1   123.490  -17.821   157948.2    9.7     70.224   1.412
 011  35.02    1.9   0.415  0.531  128480.3   33.5   39.1   123.470  -17.834   155709.8   16.6     70.771   1.959
 012  35.06    1.5   0.418  0.589  127241.1   33.8   39.4   123.450  -17.847   153424.0   16.9     72.072   3.259
 013  35.10    1.6   0.420  0.647  126010.6   31.6   36.8   123.430  -17.860   151176.1   16.1     71.492   2.680
 014  35.14    0.6   0.424  0.712  124686.1   28.8   33.6   123.409  -17.874   148779.8   14.9     76.990   8.177
 015  35.18   -0.5   0.426  0.769  123518.8    2.6    3.1   123.391  -17.886   146723.0    1.4     66.217   2.595
 016  35.22    0.1   0.428  0.828  122331.9   32.3   37.6   123.372  -17.898   144647.6   17.2     67.518   1.294
 017  35.26    4.1   0.431  0.853  121947.0   30.3   35.3   123.364  -17.903   143884.2   16.2     26.125  42.688
 018  35.30    0.3   0.434  0.954  120035.3   21.6   25.1   123.334  -17.923   140608.2   11.8    108.652  39.839
 019  35.34    2.5   0.435  0.988  119355.5   83.4   97.1   123.325  -17.929   139501.1   45.9     36.134  32.678

Station 2
LogFile:            '20011118.LOG'
StationDirectory: 'C:\METREC3.5\DATA2\LCC3\'
AppearanceDate: 2001/11/18
AppearanceTime: 18:36:33
RefStarFilename: 'C:\METREC3.5\DATA2\LCC3\20011118\20011118.ref'
INFFilename: 'C:\METREC3.5\DATA2\LCC3\20011118\183633.INF'
FrameCount: 18

!                           Position          Altitude (m)          SubPoint        Dis. to Camera (m)  Velocity (Km/s)
!###   Time  Bright      x      y         h       ±h    ±pos    lon (°)   lat (°)    Dis. Cam.   ±D2C       v       ±v
 001  33.64    0.7   0.476  0.337  124223.3   35.4   44.0   123.398  -17.884   138996.6   21.0    -------  ------
 002  33.68    1.3   0.464  0.354  123109.8   21.4   26.6   123.379  -17.897   137048.0   12.9     67.014   3.555
 003  33.72    1.2   0.451  0.372  121888.6   49.9   61.9   123.359  -17.909   134986.5   30.4     70.957   0.388
 004  33.76    0.5   0.437  0.391  120786.5   27.5   34.2   123.340  -17.923   133040.2   17.0     70.232   0.337
 005  33.80    0.4   0.423  0.411  119614.3   25.2   31.3   123.320  -17.935   131089.8   15.8     69.718   0.851
 006  33.84    0.3   0.408  0.432  118362.5    0.5    0.6   123.300  -17.948   129063.0    0.3     73.128   2.559
 007  33.88   -0.1   0.393  0.453  117197.1    9.5   11.8   123.280  -17.961   127174.2    6.2     70.160   0.409
 008  33.92   -0.3   0.377  0.476  115960.6   19.0   23.5   123.259  -17.975   125207.9   12.5     74.448   3.879
 009  33.96    0.0   0.361  0.498  114802.2   34.9   43.3   123.240  -17.988   123395.2   23.3     70.227   0.342
 010  34.00    0.3   0.344  0.522  113524.1    2.4    3.0   123.219  -18.001   121483.7    1.6     74.257   3.687
 011  34.04    0.2   0.327  0.545  112421.4   24.2   29.9   123.200  -18.013   119822.0   16.6     67.648   2.921
 012  34.08    0.0   0.309  0.571  111176.1   19.8   24.5   123.179  -18.027   118016.5   13.8     74.400   3.831
 013  34.12    0.1   0.290  0.597  110002.3   25.0   31.0   123.159  -18.040   116351.3   17.7     70.761   0.191
 014  34.16    0.4   0.272  0.624  108818.5    7.8    9.7   123.139  -18.052   114731.9    5.6     70.068   0.501
 015  34.20    0.9   0.253  0.651  107654.1    7.9    9.8   123.120  -18.065   113182.9    5.8     69.045   1.524
 016  34.24    0.9   0.232  0.680  106482.0   11.3   14.0   123.100  -18.078   111651.3    8.3     71.672   1.103
 017  34.28    1.5   0.212  0.709  105270.9   42.2   52.2   123.080  -18.090   110159.7   31.4     69.716   0.853
 018  34.32    1.3   0.191  0.738  104169.7   44.6   55.2   123.062  -18.102   108827.3   33.6     66.224   4.345
```

Figure 9 – Sample detailed altitude file (excerpt of 20011118.orb for ESA's ICC2)

Authors' address

Detlef Koschny, J. Diaz del Rio, Research and Science Support Department of ESA, ESTEC, 2200 AG Noordwijk, the Netherlands, `detlef.koschny@rssd.esa.int`.

BAA observations of the 2001 Geminids: A Preliminary Report

Neil Bone

UK-based observers had excellent conditions for the 2001 Geminids. Peak ZHR of the order of 100 was found on December 13-14.

Having been in what seems the only part of the world not to enjoy so much as a glimpse of the spectacular 2001 Leonid activity, observers in the UK put their disappointment behind them with typical resilience a few weeks later, carrying out extensive watches for the Geminids. Weather conditions were quite kind, allowing observations to be collected on all nights from 2001 December 7-8 to 14-15 inclusive. Best conditions for observers in Scotland and the north of England were found on December 12-13, whilst those in southern England had excellent skies late on December 13-14 following a cold front clearance (unusually, from the east; UK weather is more often driven by Atlantic systems from the west) towards the end of the evening. Where clear, conditions were certainly cold!

Affected by cloud and moonlight in the years since the previous well-observed return in 1999 [1], the Geminids were very well placed in 2001, with New Moon falling on December 14, and maximum expected at $\lambda_{\odot}$(eq. J2000.0) = 262.0°, corresponding to about 22^{h} UT on December 13-14 [2]. The 38 observers and three local society groups listed below provided reports totalling $182^{h}22^{m}$ watch time, during which 4170 meteors (850 sporadics, 3305 Geminids and 65 others) were recorded. These totals outstrip previous highly-successful observing runs on the shower in 1991 [3] and 1996 [4].

BAA Geminid Observers 2001:

J. Abbott, S. Beaumont, J. Bingham, N. Bone, J. Bonsor, P. Brierley, P. Carson, A. Drummond, P. Dyson, L. Entwisle, M. Fraser, D. Gavine, M. Green, C. Hall, G. Hurst, R. Johnson, J. Kemp, J. Lang, J. Latham, T. Lloyd Evans, T. McEwan, H. McGee, N. Martin, S. Martin, R. Mizon, G. Parsley, N. Quinn, J. Randall, N. Rayner, J. Shanklin, D. Smith, G. Spalding, M. Stephens (France), J. Toone, A. Vincent, P. Wayne, R. Whiting, P. Yates *Norman Lockyer Observatory AS, Wiltshire AS, Worthing AS*

Results were analyzed as previously [5] to derive sky- and radiant altitude-corrected Zenithal Hourly Rates, as presented in Table 1. Population index $r = 3.42$ was used for sporadics, $r = 2.35$ for Geminids.

Geminid activity was fairly low until late on December 11-12. By December 12-13, ZHR of the order of 50 was evident, providing healthy observed rates as the shower rose towards another broad maximum, so characteristic of recent years. ZHR stayed close to 100 for much of the night on December 13-14, apparently tailing off markedly after 5^{h} UT $\lambda_{\odot}$(eq. J2000.0) = 262.25°). Rates had fallen back considerably by December 14-15.

Estimates from experienced observers yield a mean overall Geminid magnitude +2.32 (2994 meteors) compared with +2.84 for sporadics (815 meteors). In the range from magnitude +1 and brighter, Geminids were substantially more numerous by proportion than sporadics (26.9% and 16.7% respectively). Geminid activity on December 13-14 comprised mainly meteors in the magnitude +1 to +4 bracket. The proportion of bright events was fairly similar on December 13-14 and 14-15, contrasting with the situation in 1999 [1] when bright Geminids were noticeably more common after maximum.

Table 1 – Sporadic and Geminid rates 2001.

2001 Dec. (UT)	$\lambda_\odot$	T_{eff} (Hrs)	lm	F	N_{Spo}	CHR	N_{Gem}	Radiant Alt. [°]	ZHR
$07^d22^h45^m$	255.88	1.00	5.40	–	3	11.6± 6.7	4	46.5	14.1± 7.1
$08^d21^h40^m$	256.85	1.00	6.20	–	5	7.2± 3.2	6	37.3	12.8± 5.2
22^h33^m	256.89	2.85	5.50	–	16	19.6± 4.8	11	45.2	12.8± 3.9
23^h56^m	256.95	1.27	6.20	–	6	6.8± 2.8	8	57.4	9.7± 4.0
$09^d21^h48^m$	257.87	2.00	5.00	–	3	9.5± 5.5	6	39.0	17.2± 7.0
22^h21^m	257.90	1.00	6.40	–	10	11.3± 3.6	5	44.0	7.8± 3.5
23^h29^m	257.95	2.20	6.20	–	9	5.9± 2.0	12	54.4	8.7± 2.5
$10^d01^h30^m$	258.03	1.00	6.10	–	8	13.1± 4.6	3	68.3	4.5± 2.6
02^h30^m	258.07	1.00	6.10	–	9	14.7± 4.9	5	69.9	7.5± 3.4
21^h35^m	258.88	1.00	5.20	–	5	24.7±11.0	5	37.7	24.8±11.1
23^h29^m	258.92	3.00	6.20	–	8	3.9± 1.4	19	54.7	10.0± 2.3
$11^d00^h19^m$	259.00	4.50	5.92	–	17	7.7± 1.9	34	61.5	14.1± 2.4
01^h30^m	259.05	3.05	5.83	–	17	12.7± 3.1	40	68.6	25.0± 4.0
02^h28^m	259.09	2.00	5.80	–	13	15.4± 4.3	12	68.8	11.7± 3.4
21^h21^m	259.89	3.33	5.07	–	4	7.0± 3.5	12	36.2	20.7± 6.0
22^h30^m	259.94	5.25	5.50	–	13	8.5± 2.4	33	46.6	20.3± 3.5
23^h34^m	259.98	6.00	5.96	–	28	9.1± 1.7	54	56.0	17.2± 2.3
$12^d00^h21^m$	260.01	8.12	5.71	–	41	13.3± 2.1	70	62.2	19.1± 2.3
01^h19^m	260.06	5.00	5.72	–	32	16.7± 3.0	88	68.1	36.9± 3.9
02^h39^m	260.11	5.05	6.18	–	48	14.1± 2.0	77	69.3	21.4± 2.4
03^h41^m	260.15	3.92	6.10	–	31	12.9± 2.3	53	63.4	21.3± 2.9
04^h37^m	260.19	2.00	5.70	1.09	8	11.7± 4.1	15	55.6	19.6± 5.1
05^h27^m	260.23	1.33	5.70	1.09	5	11.0± 4.9	10	49.0	21.5± 6.8
06^h25^m	260.27	0.83	6.00	–	4	8.9± 4.5	5	40.9	14.1± 6.3
21^h36^m	260.92	2.00	5.75	–	8	10.1± 3.6	21	39.2	31.5± 6.9
22^h41^m	260.96	2.00	5.75	–	4	5.0± 2.5	41	48.3	52.1± 8.1
23^h39^m	261.00	1.50	5.75	–	5	8.4± 3.8	33	55.9	50.4± 8.8
$13^d00^h34^m$	261.04	4.00	5.78	–	16	9.7± 2.4	95	62.1	49.7± 5.1
01^h33^m	261.08	3.00	5.90	–	12	8.4± 2.4	77	66.4	46.8± 5.3
02^h39^m	261.13	1.00	6.00	–	8	14.5± 5.1	24	66.2	40.2± 8.2
03^h39^m	261.17	1.00	6.00	–	4	7.4± 3.7	29	61.8	50.4± 9.4
04^h27^m	261.21	2.00	5.80	–	9	10.6± 3.5	61	56.4	66.6± 8.5
05^h28^m	261.25	1.77	5.70	–	8	12.1± 4.3	43	48.3	64.5± 9.8
23^h40^m	262.02	2.58	5.50	1.17	5	7.8± 3.5	84	58.3	105.2±17.5
$14^d00^h19^m$	262.05	4.33	5.49	1.05	17	14.3± 3.5	164	64.1	104.8± 8.2
01^h21^m	262.09	4.83	5.81	1.02	33	16.3± 2.8	229	69.7	93.0± 6.1
02^h26^m	262.14	5.97	5.51	–	36	20.4± 3.4	232	70.5	96.1± 6.3
03^h26^m	262.18	7.00	5.74	1.06	41	15.8± 2.5	313	65.5	99.7± 5.6
04^h26^m	262.22	6.00	5.79	1.10	47	20.6± 3.0	235	57.6	93.6± 6.1
05^h18^m	262.26	4.55	5.78	1.10	42	24.6± 3.8	138	49.9	80.7± 6.9
06^h08^m	262.30	2.00	6.40	–	19	10.7± 2.5	87	42.2	70.5± 7.6
21^h30^m	262.95	2.75	5.75	–	7	6.4± 2.4	14	39.2	15.3± 4.1
22^h31^m	262.99	1.87	6.17	–	8	6.4± 2.3	11	48.6	10.4± 3.1
23^h22^m	263.03	7.68	5.68	–	20	7.1± 1.6	78	55.9	24.7± 2.8
$15^d00^h20^m$	263.07	5.00	5.85	–	21	9.3± 2.0	65	64.2	25.2± 3.1
01^h18^m	263.11	2.00	5.63	–	14	20.4± 5.5	21	70.6	23.4± 5.1
02^h30^m	263.16	1.00	5.25	–	4	1.5± 6.8	11	71.0	33.8±10.2

Some notable Geminid fireballs were reported. An exploding Geminid, flaring to as bright as magnitude −7 was reported at 02^h59^m UT on December 13-14 by Alan Drummond (Sussex), Nigel Rayner (Essex), George Spalding (Oxfordshire) and Jonathan Shanklin (Cambridge). John Toone in Cheshire reported a magnitude −5 Geminid lighting up sky and ground at 4^h26^m UT on December 13-14; this was also seen by Jim Latham in North Wales. Guy Hurst in Hampshire saw a slow magnitude −5 event at 6^h38^m UT at the end of the same night.

A group at the *Norman Lockyer Observatory (NLO)* in Devon saw a blue-green magnitude −10 Geminid on December 14-15 at 21^h07^m UT; this was also reported by Stephen Martin elsewhere

in Devon. The *NLO* observers reported a second, magnitude −6 event, at 21^h08^m UT on a similar path. Perhaps the most widely seen event came at 0^h01^m UT on December 14-15, variously reported at magnitude −2 to −6 by observers from Devon and North Wales to Sussex, Kent and Cambridge.

As in past years, comparatively few Geminids (101/2839 = 3.6%) showed persistent trains relative to the contemporaneous sporadic background (69/772 = 8.9%).

Thanks are, as ever, expressed to all observers who contributed to the success of this observing campaign.

References

[1] N. Bone, *WGN* 28:5, 2000, pp. 183–184.
[2] "BAA Handbook", 2001.
[3] S.J. Evans, N.M. Bone, *J. Brit. Astron. Assoc.* 103:6, 1993, pp. 300–304.
[4] S.J. Evans, N.M. Bone, *J. Brit. Astron. Assoc.* 111:1, 2001, pp. 33–37.
[5] N. Bone, *WGN* 22:2, 1994, pp. 77–79.

Author's address

Neil Bone, "The Harepath", Mile End Lane, Apuldram, Chichester, West Sussex, PO20 7DZ, UK, e-mail: `neil@bone2.freeserve.co.uk`.

The Leonid 2001 Project by Radio Meteor Observations All over the World

Hiroshi Ogawa, Shinji Toyomasu, Kouji Ohnishi, and Kimio Maegawa

In 2001, the Leonid meteor shower was expected to be a great event in America, Asia, and Australia. Therefore, it was important to catch the signature of the outburst and monitor the whole Leonid activity. Radio meteor observations are one of the best methods for monitoring meteor activity because it is possible to observe even if in bad weather or at daytime. Moreover, by considering the radiant elevation, we succeeded in monitoring the whole Leonid activity. In addition, by using a relative quantity, it became possible to unify world-wide data. In this research, by using data of radio meteor observations all over the world, we analyzed the 2001 Leonid activity. As a result, two clear peaks were observed and we succeeded in observing the whole Leonid activity.

1. Introduction

In 2001, a Leonid meteor storm was expected to show the greatest appearance in recent years. Some researchers published predictions [1,2,3]. Therefore, it was important to monitor the whole Leonid activity. One of the best methods for monitoring meteor activity is radio meter observing because it is possible to observe even if in bad weather or at daytime. At only one site, however, we may miss the Leonids' main peak due to low radiant elevation. Therefore, we unified world-wide data of radio meteor observations, and it became possible to monitor the activity without this problem. The unification of world-wide data, however, has a serious problem. It is the differences of observational equipment and geographical conditions. To solve this problem, comparable data were calculated by a relative quantity. Consequently, by using the relative quantity after confirmation of its effectiveness, the Leonid meteor activity was analyzed. To observe the whole Leonid activity, we planned "The Leonid 2001 project by radio meteor observations all over the world" [4]. Then, 91 sites in 15 countries participated. In this research, we visualized the whole Leonid activity by radio meteor observations all over the world.

2. Activity Level

Each observer reported the number of meteor echoes every hour. To observe the whole Leonid activity, the unification of world-wide data was needed. However, since observational equipment (e.g. frequency, antenna pattern, etc.) and geographical conditions (e.g. distance between transmitting and receiving station) are different, it is difficult to unify and compare these data. In this Paper, therefore, a new index of "Activity Level" was used. This index is calculated by the following formula.

$$A_{\mathrm{site}}(t) = \frac{H - H_0}{H_0}$$

$$A(t) = \frac{\sum_{i=1}^{N} A(t)_{\mathrm{i}}}{N}$$

$A(t)$ means the new index, the "Activity Level". H is the number of echoes for a certain hour. H_0 is the number of background echoes during two weeks, which were defined by observational data from November 1 to 13. Therefore, $A_{\mathrm{site}}(t)$ means how many times are echoes observed compared to the background echo rate. Then each $A_{\mathrm{site}}(t)$ is calculated at each site, and $A(t)$ is the average of all $A_{\mathrm{site}}(t)$. N is the number of observational sites. If there is no meteor shower activity, $A(t)$ is around 0. Figure 1 is the result of this calculation for January 2001. These data were provided by five sites.

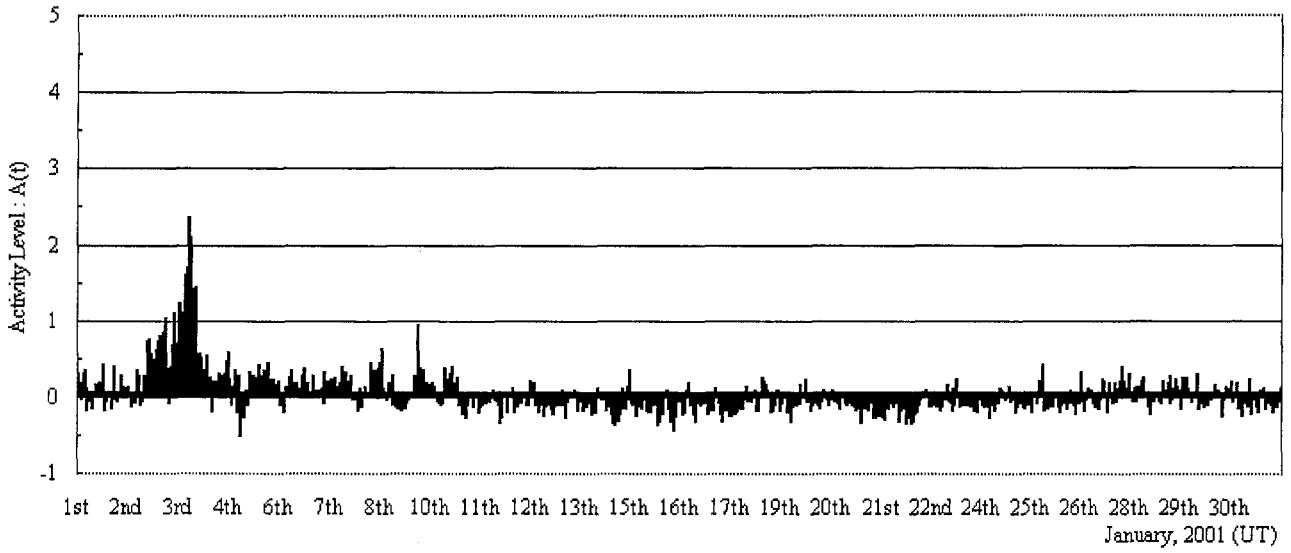

Figure 1 – The result by using the $A(t)$ formula in January 2001. The observers were as follows: Bruce Young (Australia), Stan Nelson (USA), Dave Swan (UK), Pierre Terrier (France), Misato Observatory (Japan).

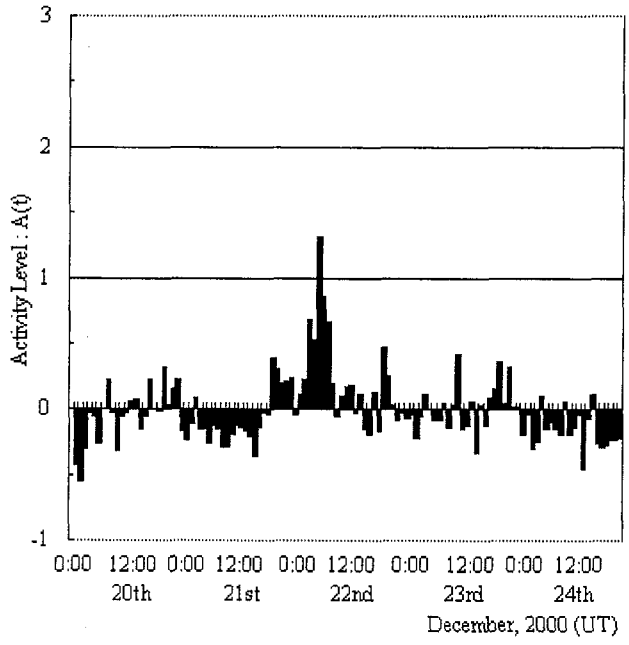

Figure 2 – The 2000 Ursids by radio meteor observations. The observers were as follows: Bruce Young (Australia), Stan Nelson (USA), Dave Swan (UK), Pierre Terrier (France), Misato Observatory (Japan).

This result shows the Quadrantid activity around January 3. At that time, the maximum $A(t)$ was 2.6. Therefore, this method is applicable for observing the activity of meteor showers. Also the outburst of the 2000 Ursids was observed [5]. Figure 2 shows this result. Obviously, this method can also observe an outburst. Other meteor showers were also analyzed by this method. The maximum value of the Geminids in 2000 was 3.8, that of the Lyrids in 2001 was 0.8, and the average in February 2000 (no-main meteor shower activity) was 0.01.

Consequently, this value shows the meteor activity clearly and it is effective and applicable for monitoring meteor activity. In 2001, by using this method, we monitored and analyzed the Leonid meteor activity.

3. Leonid 2001 Project

To observe the whole Leonid activity, we planned the "Leonids 2001 project by radio meteor observation all over the world". Ninety-one sites in 15 countries participated. In particular, there were many sites in Japan (77 sites). Figure 3 shows two maps of the participants. This project started on November 1. Then, the background level was defined from November 1–13. Since November 14, flash reports and live reports of the observed data were issued every day. In particular, the live reports were updated every 10 minutes. After the Leonid activity had finished, a lot of observational data were reported. These data were updated on a home page, and everybody is invited to use these data (`http://homepage2.nifty.com/~baron/database.htm`).

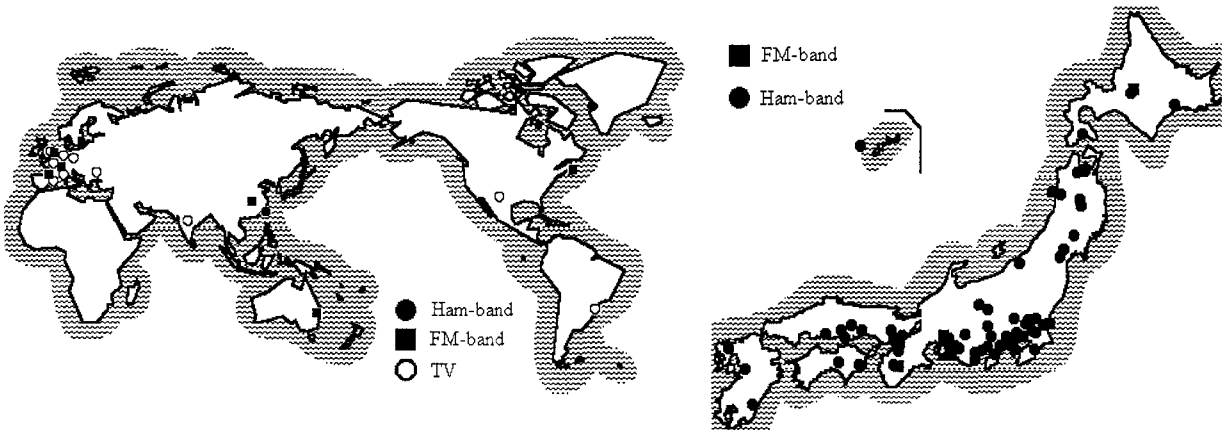

Figure 3 – Site map of participants in the Leonid 2001 project in the world (top) and in Japan (bottom).

The participants were the following:

Pierre Terrier (France), Jean Marie Polard (Belgium), Ton Schoenmaker (the Netherlands), Dave Swan (UK), Syd (UK), Didier Favre (France), Udo Langenohl (Germany), Stan Nelson (USA), Michael Boschat (Canada), Rafael Haag (Brazil), Bruce Young (Australia), Garfield TSAO (Taiwan), Ouyang Tianjing (China), Aundhkar Shrinivas (India).

Japan: Kenichi Shibata, Tetsuharu Sasaki, Toshiro Sato, Masayuki Yamamoto, Kunihiko Nakano, Hitoshi Kitazume, Yoshiharu Ito, Hironobu Sida, Masayuki Kobayashi, Kazuyuki Nagao, Yoshio Kimura, Minoru Ehara, Yoichi Okamoto, Masaru Hasegawa, Hirofumi Sugimoto, Takuya Ogawa, Masami Kurihara, Chikara Yamaguchi, Yuka Masui, Toshihiko Masaoka, Seiji Fukushima, Tomohiro Koiwa, Masayuki Nagase, Toshiaki Tsuruoka, Yosuke Utsumi, Yukio Abe, Chiaki Kato, Hiroshi Nakano, Hitoshi Yadotani, Takashi Usui, Manichiro Isigooka, Isamu Ohmori, Izumi Saito, Kouji Ohnishi, Satoru Suzuki, Takashi Asahina, Kazuhiro Suzuki, Sadao Okamoto, Takumi Yata, Ryo Ishii, Kayo Miyao, Koichi Kimura, Masayoshi Ueda, Yoshiyuki Hamaguchi, Kimihiro Norizawa, Yoshikazu Kato, Toshihide Miyake, Koji Maeda, Kazuhisa Kageyama, Taisuke Kondo, Kenichi Fushimi, Yukio Ichikawa, Iai Girls' Senior and High School, University of Tsukuba, Ibaraki-NCT, Hoshino Girls' High School, Koshigaya-Kita High School, Ueda High School, Nagano-NCT, Mikawa Junior High School (Eiji Kubota), Damine Meteor Observatory, Asahigaoka High School, Kato Gakuen Shoto School, SHOYO High School, Kyoto Sangyo University (Taku Nakajima), Hoshinoko-Kan (Ohmi Iiyama), Nishi Harima Observatory (N. Tokimasa and M. Yamamoto), Misato Observatory (Shinji Toyomasu), Okayama-Asahi High School, Fukuyama Junior and Senior High School (Hiroyuki Hiraga), Awa High School.

4. Results

Figure 4 shows the result of the whole Leonid activity period from world-wide data. The vertical axis is the "Activity Level ($A(t)$)". Three curves mean the radiant elevations in the USA, in the UK, and in Japan. In the Leonid analysis, only data for which the radiant elevation is between 20° and 80° were used, and the same factor as for visual observations, $1/\sin h$ (h: radiant elevation) was applied as a correction. In addition, the elimination of erroneous outliers was applied, which defines that $A(t)$ within $\pm 1.5\sigma$ comprises useful data. Since there were many sites in Japan, it is divided into five areas.

We found two clear peaks around $10^{\rm h}$UT and $18^{\rm h}$ UT on November 18. High activity became obvious at $3^{\rm h}00^{\rm m}$ UT on November 18. Around $5^{\rm h}00^{\rm m}$ UT, the Leonid activity became higher and higher. Figure 5 is an illustration for the period around the main peak.

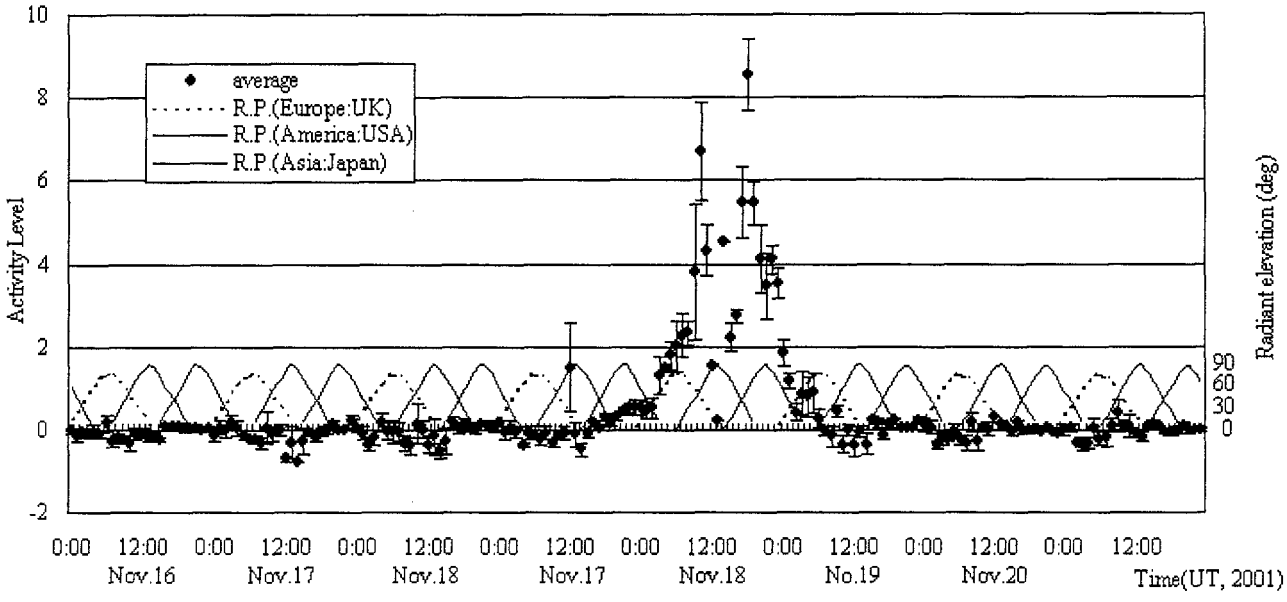

Figure 4 – The Leonids' whole activity from radio meteor observations. Observers are as follows: Bruce Young (Australia), Rafael Haag (Brazil), Michael Boschat (Canada), Pierre Terrier (France), Ton Schoenmaker (the Netherlands), Dave Swan (UK), Stan Nelson (USA), Takashi Asahina (Japan), Isamu Ohmori (Japan), Ken-ichi Fushimi (Japan), Kazuhisa Kageyama (Japan), Takumi Yata (Japan), Koichi Ishitani (Japan), Hirofumi Sugimoto (Japan), Toshihide Miyake (Japan), Asahigaoka High School (Japan), Nishi-Harima Observatory (Japan), Toshihiko Masaoka (Japan), Okayama-Asahi High School (Japan), Yoshiharu Ito (Japan), Kayo Miyao (Japan), Chiaki Kato (Japan), Ken-ichi Shibata (Japan), Hironobu Shida (Japan), Kazuyuki Nagao (Japan), Seiji Fukushima (Japan), Tetsuharu Sasaki (Japan), Ueda High School (Japan), Tomohiro Koiwa (Japan), Hideo Nakanishi (Japan), Awa High School (Japan),Hitoshi Yadotani (Japan).

The maximum $A(t)$ of the American peak was 6.7 ± 1.2 and that of the Asian-Australian peak was 8.5 ± 0.9. Around the Asian-Australian peak, however, the value of $A(t)$ was not certain. As a reason of uncertainness, we found that it was difficult to count the number of meteors because the number of long echoes increased. Therefore, the true $A(t)$ of the main peak would be much higher than this result. Figure 5 also shows a result similar to the report by *The International Meteor Organization (IMO)*. The first peak corresponded to the American peak with a ZHR of 1620 at $10^{\rm h}39^{\rm m}$ UT on November 18, and the second peak was the Asian and Australian peak with a ZHR of 3430 at $18^{\rm h}16^{\rm m}$ UT on November 18 [6]. According to a few of the predictions, the American peak corresponded to the 7-revolution dust trail and the Asian and Australian peak was caused by the 4-revolution and 9-revolution dust trails (it was impossible to divide the main peak into two dust trail components). The half-width time of the American peak was about ±90 min, and that of the Asian-Australian peak was about −180 min/ + 240 min. Also, Figure 5 indicates a sub-peak around $21^{\rm h}$ UT on November 18.

5. Discussion and conclusion

In this study, we observed two clear peaks. One peak was the American peak around 10^h on November 18, the other peak was at 18^h on November 18 in Asia and Australia. The half-width time was ± 90 min in America and -180 min/ $+ 240$ min in Asia and Australia. Given that the revolution velocity of the Earth is 30 km/s and the orbital inclination of the parent comet is 163°, the lengths through the dust trails was 9.5×10^4 km for the American peak and 2.2×10^5 km for the Asian and Australian peak. In particular, this value for the Asian and Australian peak is much longer than some predictions estimated [2,3]. Also, a sub-peak around 21^h UT was observed. This appears to be the reason for the remaining high activity reported by Japanese visual observation [7]. On the other hand, by using the $A(t)$ index, it is possible to monitor the meteor activity at all times. Therefore, a monitoring like this project is not expected only during the Leonid meteor shower, but also for the annual meteor activity.

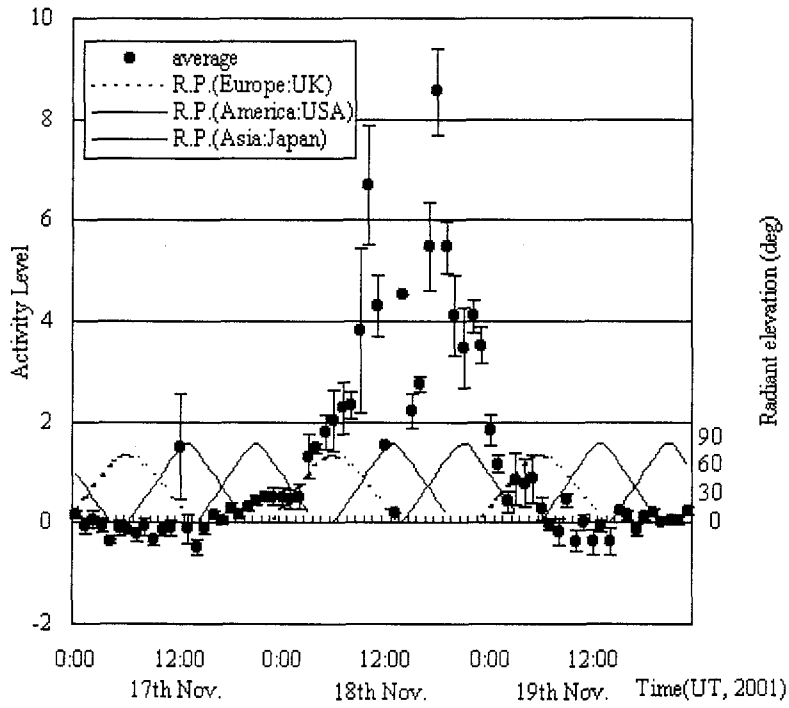

Figure 5 – The Leonid activity around the main peak.

References

[1] R.H. McNaught, D.J. Asher, "Leonids dust trails and meteor storms", *WGN* 27 (1999), pp. 85–102.

[2] E.J. Lyytinen, "Prediction the strength of Leonids outburst", *Earth, Moon and Planets* 82 (2000), pp. 149–166.

[3] E.J. Lyytinen, M. Nissinen, T. van Flandern, "Improved 2001 Leonids Storm Predictions from a Refined Model", *WGN* 29 (2001), pp. 110–118.

[4] H. Ogawa, S. Toyomasu, K. Ohnishi, K. Maegawa, "Leonids 2001 Project by Radio Meteor Observation All Over The World", `http://homepage2.nifty.com/~baron/leo01p.htm`, 2001.

[5] P. Jenniskens, E.J. Lyytinen, "2000 Ursids Outburst Confirmed", *WGN* 29 (2001), pp. 41–45.

[6] R. Arlt, J. Kac, V. Krumov, A. Buchmann, J. Verbert, "Bulletin 17 of the International Leonids watch: First Global Analysis of the 2001 Leonids Storms", *WGN* 29 (2001), pp. 187–194.

[7] H. Ogawa, S. Uchiyama, " The 2001 Leonids Meteor Storm over Japan", *WGN* 29 (2001), pp. 206–213.

Authors' addresses

Hiroshi Ogawa, The Nippon Meteor Society, 36-47 Nakane, Kutsukake, Toyoake, Aichi, 470-1101, Japan, e-mail ogawa@nms.gr.jp.

Shinji Toyomasu, Misato Observatory, 180 Matsugamine, Misato, Kaiso, Wakayama, Japan, e-mail toyomasu@obs.misato.wakayama.jp.

Kouji Ohnishi, Nagano National College of Technology, 716 Tokuma, Nagano, Nagano, 381-8550, Japan, e-mail ohnishi@ge.nagano-nct.ac.jp.

Kimio Maegawa, Fukui National College of Technology, Geshi, Sabae, Fukui, 916-8507, Japan, e-mail kmaegawa@fukui-nct.ac.jp.

Erratum on

SPA Meteor Section Results: 2001 Leonids

Alastair McBeath

Unfortunately, the headers of the graphs in Figure 6 were cropped upon editing the article. We would like to apologize for the inconvenience and repeat the full Figure—Ed.

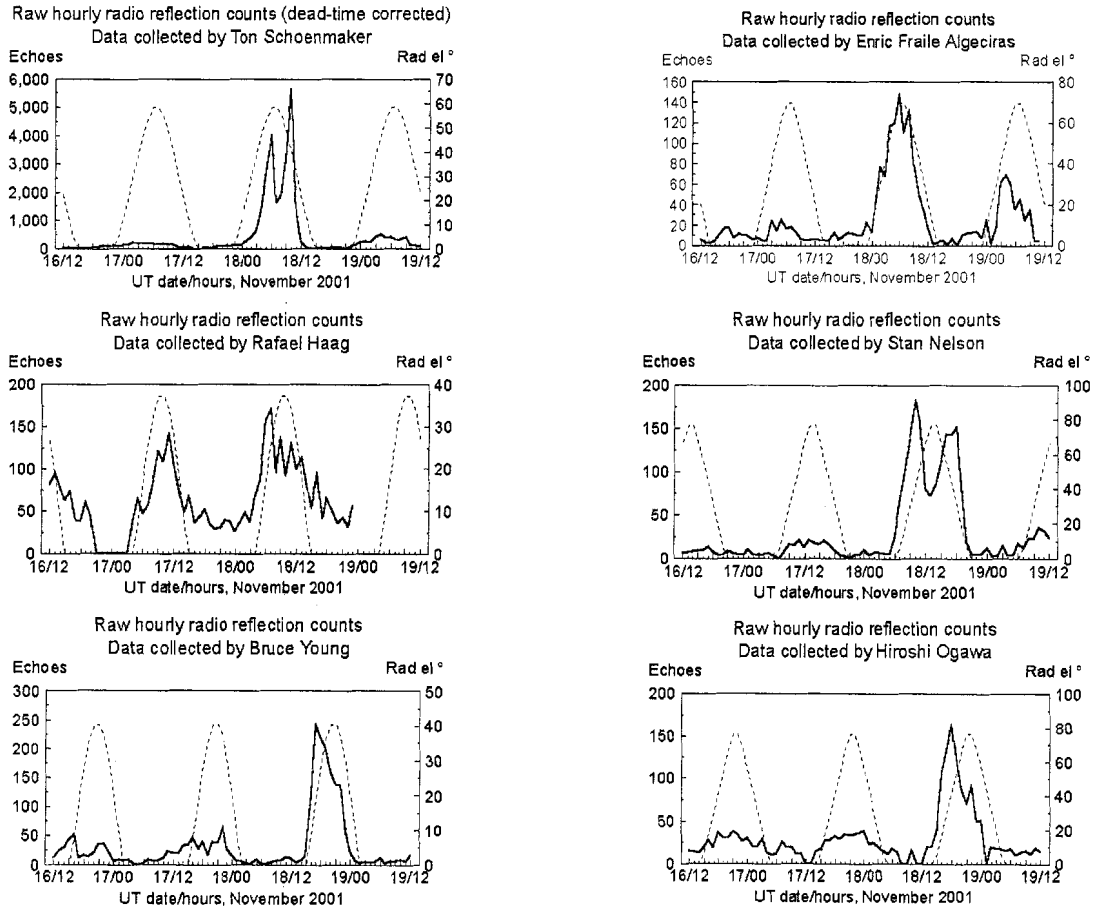

Figure 1 – Six graphs showing raw radio meteor echo counts, as collected by the stated observers, from midday UT on November 16 to midday UT on November 19 (thicker, irregular lines, keyed to the left-hand y-axes). The finer, symmetrical lines, keyed to the right-hand y-axes, give the Leonid radiant elevation in degrees for each observer's site. Ton Schoenmaker's data is corrected for dead time due to his system being saturated by meteor echoes where more than 10to this cause.

On the Presence of Persistent Trains in Leonid Fireballs from 1998, 1999 and 2000 Spanish Meteor Observations

Orlando Benítez Sánchez

The properties of Leonids and its persistent trains produced from fireballs are investigated with visual records carried out by SOMYCE members from 2616 fireballs brighter than visual magnitude −2 which left 663 persistent trains of known duration. The "population index", τ, for the train distribution in 1998 was $\tau = 0.838 \pm 0.053$ for the interval [$\leq$ 0.5 s, 8 s], $\tau = 0.979 \pm 0.010$ for the interval [10 s, 30 s], and $\tau = 0.995 \pm 0.049$ for the interval [35 s, 600 s]. In 1999, τ was lower: $\tau = 0.468 \pm 0.166$ for the interval [0.5 s, 7 s], while in the 2000 data, similar values as from the 1998 observations are found with $\tau = 0.976 \pm 0.255$ for [$\leq$ 0.5 s, 150 s]. These values are greater than the usual ones of sporadic fireballs with 0.67 ± 01

1. Introduction

It is well known by meteor observers that after the passage of a meteor body, sometimes we may distinguish some characteristic region, called train or persistent train.

These regions are detectable due to some characteristic processes, as ionization and light emission, which can be observed visually and photographically.

A good review about the physics of this phenomena can be read in *WGN* 20:3 (Bellot Rubio, 1992). That article shows that in short-lived train, the electric neutralization between positive meteoritic ions and negative atmospheric ions are the most important mechanisms, while for long-lived trains, it is the recombination processes of atoms and molecules behind the meteor. It is not yet well known, but it seems that two important recombination processes are between atomic nitrogen and the sodium catalytic cycle.

2. Observational data characteristics

In this study, 2615 fireballs are analyzed to get the visual train rates for the fireball component of the Leonid meteor shower in 1998, 1999, and 2000 from Spanish observations forwarded to SOMYCE. A summary of the observers who have contributed to this study is as follows:

Pedro Aguilera Moreno, Ander Aizpuru, Raquel Álvarez Franco, Clossan Andrade, Arnaldo Arnal, Luis R. Bellot Rubio, Rafael Benavides Palencia, Orlando Benítez, Antonio Bernal González, Rafael Benavides Palencia, Miguel Ángel Bennasar, Mikel Berrocal, Juana Brunet, Luis M. Castro Vozmediano, Diego Cerro Ferreira, Javier Campos, Alberto Carrillo, Antonio Company, Jose Chambó, Rubén Darío Ramos, Matías Dávila, Silvia Díez Smith, Matías Domínguez, David Fernández Barba, Ricardo Fernández, Enric Fraile Algeciras, Fernando García Martín, Faustino García de la Cuesta, Juan Andrés García Escusa, Lucas Gil Peruzzotti, Diego Giraudi, Juan R, Gómez, Diego Gómez Palacio, Jordi González, Pedro Luis González, Oswaldo González Sánchez, Jose Luis Guixeras, Antonio Gutiérrez Corrales, Carles Gutierrez, Carlos Hernández, David Hernández Ojados, Rafaél Juárez, Jaime Hodra, Manuel Jiménez del Barco, Mark Kidger, Jesus Leal Castro, Ángel R. López, Antonio E. López Blanco, Ángel López Postigo, Charo Lozano, Fernando López La Puente, Edgardo Rubén Masa Martín, David Martínez Delgado, Antonio Martínez Torres, David Martínez Delgado, Ángel E. Milara, Isabel Nieto, Francisco Ocaña González, Federico Pardavila, Vicent Peris, Carles Pineda, Dulce Placencia, Francisca Quetglas Jaime Resino, Francisco Reyes Andrés, José Ripero, Orlando Rodríguez, Francisco Alberto Rodríguez, Gabriel Rodríguez, Sergio Iván Rodríguez, Jesús Gerardo Rodríguez, Juán Rodríguez, Antonio Román Reche, Julián Ruiz-Garrido, Victor Ruiz, Ángel Rafael Sánchez López, Francisco Sáez, Luis Salas, Sergio Sánchez Jiménez, Javier Sánchez Portero, Ginés Segovia Muñon, Miguel Angel Serra Martín, Miguel Serra Ricart, Francisco Sevilla Lobato,, Manuel Sirvent, Manuel Solano, José María Soria, Máximo Suárez, Eduardo Svaikauska, Josep M. Trigo, Carlos Vera Hernández, Daniel Verde van Ouytsel, Miguel Antoni Villalonga, Bruno Vanrell, Cristina Willem.

Agrupación Astronómica de Gran Canaria, Agrupación Astronómica Tamix, Agrupación Astronómica Turolense Actuel, Grupo de Estudios Astronómicos de Puertollano, Observatorio Astronómico de Mallorca, Sociedad Astronómica de Castellón y la Sociedad Astronómica de Zaragoza.

The majority of fireballs were observed in the morning of November 17-18, except the fireball maximum of November 16-17 in 1998. The relevant data are shown in Table 1.

Spanish observers registered 22938 Leonids and 2839 visual trains. The presence of trains was not indicated by all the observers, so in this study, only 663 trains have been used. Detailed data for 1998, 1999, and 2000 observations are shown in Table 1.

Table 1 – Total Leonid numbers and fireball observations carried out by SOMYCE members on 1998, 1999, and 2000. Fireball percentages refer to the total number of Leonids, and train percentages refer to the fireball number.

Year	Leonids	Fireballs	Persistent trains	% Fireballs	% Fireball trains
1998	3548	1189	324	35.51	27.25
1999	15995	1127	248	7.04	22.02
2000	3395	300	91	8.84	30.33

The duration of a meteor train usually is less than 10 seconds. The visual observation, i.e. recorded on a tape, requires exceptional concentration and quick reaction on the part of the observer to catch, at the same time, several meteors if the activity is high; however, for shorter durations, trains data use to be quite accurate. For longer-duration trains, we expect a very different situation, and if we want the exact duration of visibility, it may be that we will have to make a break in the observation, so that is not the usual situation, and the data show "breaks" around certain rounded values, like, 10, 15, 25, or 60 seconds. For that reason, we expect that the accuracy of long-lives trains (> 60 sec) should be only an approximation.

The distribution of trains is represented graphically versus frequency (in normalized values calculated as the number of persistent trains divided by the total per magnitude class)

By comparison, we observe that in 1999 and 2000, the fireballs rates were lower than in 1998, so the presence of persistent trains associated with bright fireballs is less important.

In 1999 and 2000, the shorter trains have low frequency values in comparison with 1998. That indicates a smaller general size of particles than in 1998, where the fireball shower was evident.

In fact, the largest frequencies are always associated with the brightest fireballs. The coefficient of perception has its maximum value, unity.

3. Relationship between the number of trains and their duration time: τ

This relation is similar to that existing between the number of meteors and their magnitude, whence we can speak of a "population index", τ, for the train distribution. The computation is quite analogous to the population index, r, although it is necessary to include some variations. First, we choose a maximum duration to start the procedure, in our case, we chose 1200, 60, and 150 seconds for the 1998, 1999, and 2000 observations, respectively.

Then, the cumulative number of trains must be calculated from longer to shorter durations, as the number of trains increases with decreasing duration. Finally, we expect a relation of the form:

$$\Phi(T) = 10^{aT+b}, \tag{1}$$

where $\Phi(T)$ is a cumulative number of trains of at least T seconds, and a and b are constants. Then, the "population index" τ is given by $\tau = 10^a$, or in other terms, we can write

$$\Phi(T+1)/\Phi(T) = \tau,$$

i.e., on average, there are τ times as many trains with life at least $T+1$ second that there are trains with duration at least T seconds.

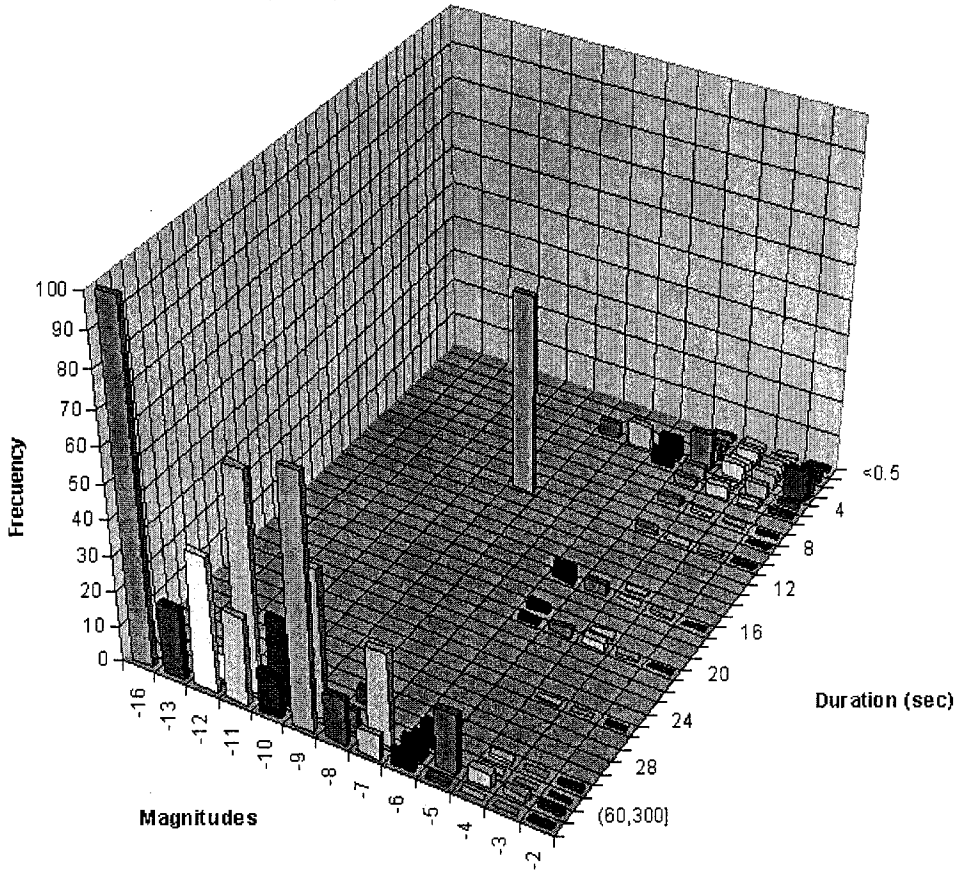

Figure 1 – Train distribution for the 1998 observations. For longer durations the data have a large dispersion and were grouped in intervals.

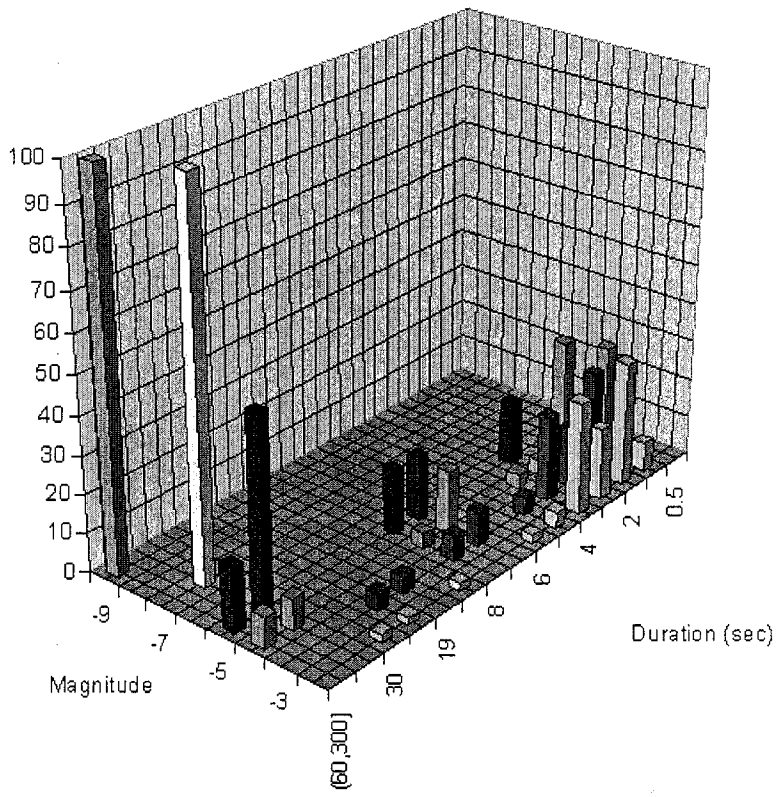

Figure 2 – Train distribution for the 1999 observations.

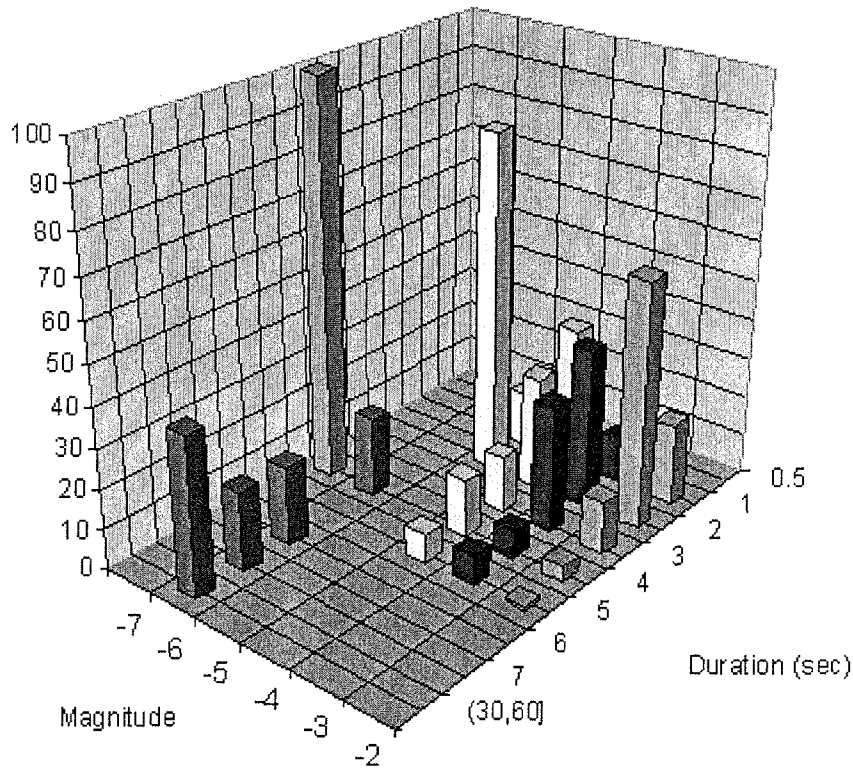

Figure 3 – Train distribution for the 2000 observations.

The calculations have been carried out for the entire observing period for each year. A typical error for τ is estimated. Leonid fireballs and their persistent train are an obvious event, so we suppose that the perception coefficient, P, is equal to unity. The results are summarized in Table 2.

Table 2 – Results obtained in different intervals for which high correlation r^2 was found. The fits of a and b refer to Equation (1); $\tau = 10^a$.

Year	Interval	b	a (slope)	r^2	τ	Error
1998	[≤ 0.5, 1200]	2.013	−0.002	0.832	0.995	0.237
	[≤ 0.5, 8]	2.558	−0.077	0.945	0.838	0.053
	[10, 30]	2.090	−0.009	0.980	0.979	0.010
	[35, 600]	1.869	−0.002	0.986	0.995	0.049
1999	[0.5, 7]	2.776	−0.330	0.962	0.468	0.167
	[2, 7]	3.094	−0.340	0.990	0.460	0.100
	[0.5, 30]	1.880	−0.064	0.610	0.863	0.616
2000	[≤ 0.5, 8]	2.057	−0.110	0.962	0.776	0.062
	[21, 150]	1.295	−0.007	0.899	0.984	0.133
	[0.5, 150]	1.566	−0.010	0.770	0.977	0.255

4. Graphical description and comparison.

A cumulative function is presented versus the train duration in seconds (Figure 4). Logarithmic axes were plotted to identify a linear relation. The 1998 observations are well covered in the full duration interval, but it seems that the data show different linear relations in the three intervals [≤ 0.5 s, 5 s], (5 s, 300 s], and (300 s, 800 s]. The last interval, 300 s to 800 s has been used

to determine the experimental limiting train duration in a visual observation, to prolong the correlation regression to the x-axis. That duration is about 3000 seconds (50 minutes). Similar relations are found for both years, 1999 and 2000 observations, with a clear convergence around that duration.

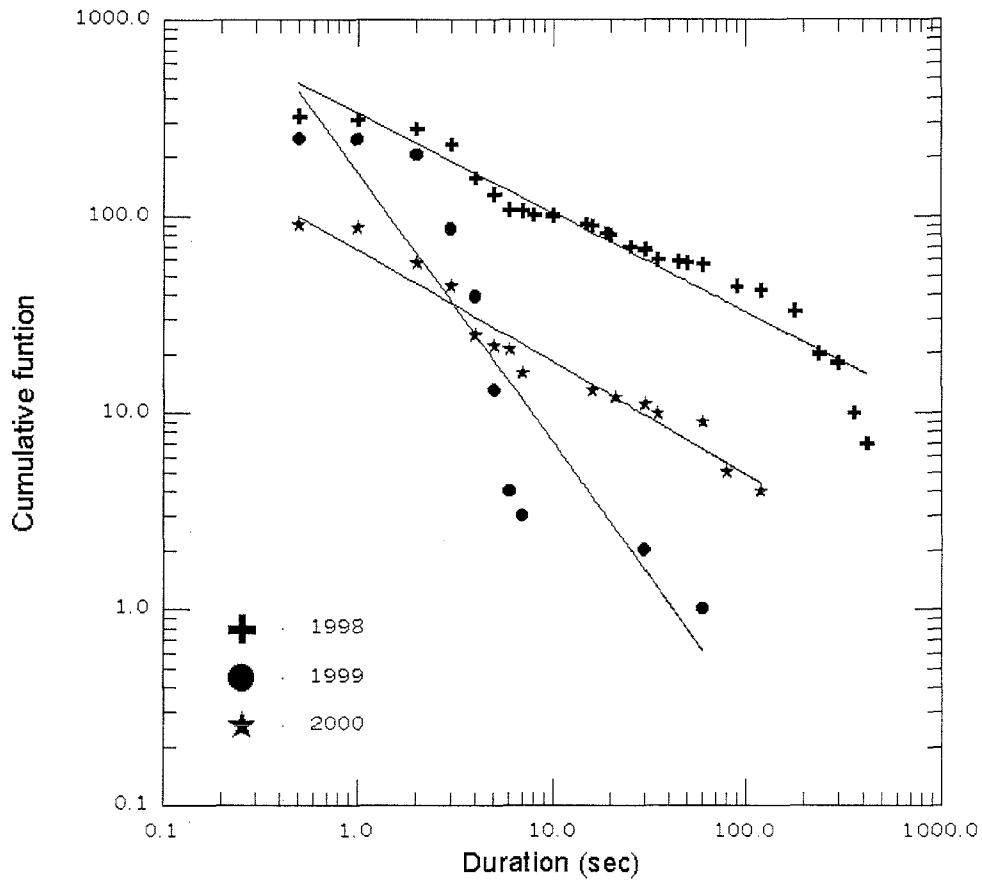

Figure 4 – The cumulative numbers Φ versus persistent train duration T in double-logarithmic plot. The straight lines indicate that also a power-law could be a reasonable description of $\Phi(T)$.

The linear regression by all the data have a good determination coefficient, r^2, in particular for 1998 thanks to the experienced data from Mallorca and Canary Islands observers.

In 1998 and 2000, the slope is quite similar, but not in 1999 with $\tau = 0.486 \pm 0.167$ for the interval [$\leq$ 0.5 s, 7 s]. It is evident that the observed fireball rates are an important factor, but as we said before, if the perception is 100%, we affirm that in 1999 the trains had a different evolution.

Comparing this value with those of fireballs and annual showers shown in Bellot Rubio (1992), all τ values of Leonids are greater than the value of sporadic fireballs ($\tau = 0.67 \pm 0.01$) [2].

For the Perseids, τ was 0.33 ± 0.02, for the Orionids, $\tau = 0.22 \pm 0.03$, and for the sporadic background, $\tau = 0.36 \pm 0.02$.

5. Photographic observations

About 500 meteors have been photographed by SOMYCE members. On about 50 different negatives, persistent trains were registered. Meteor trains are usually linear, but a significant number have been reported to be non-linear when the dissipative effect of the upper atmosphere occurs.

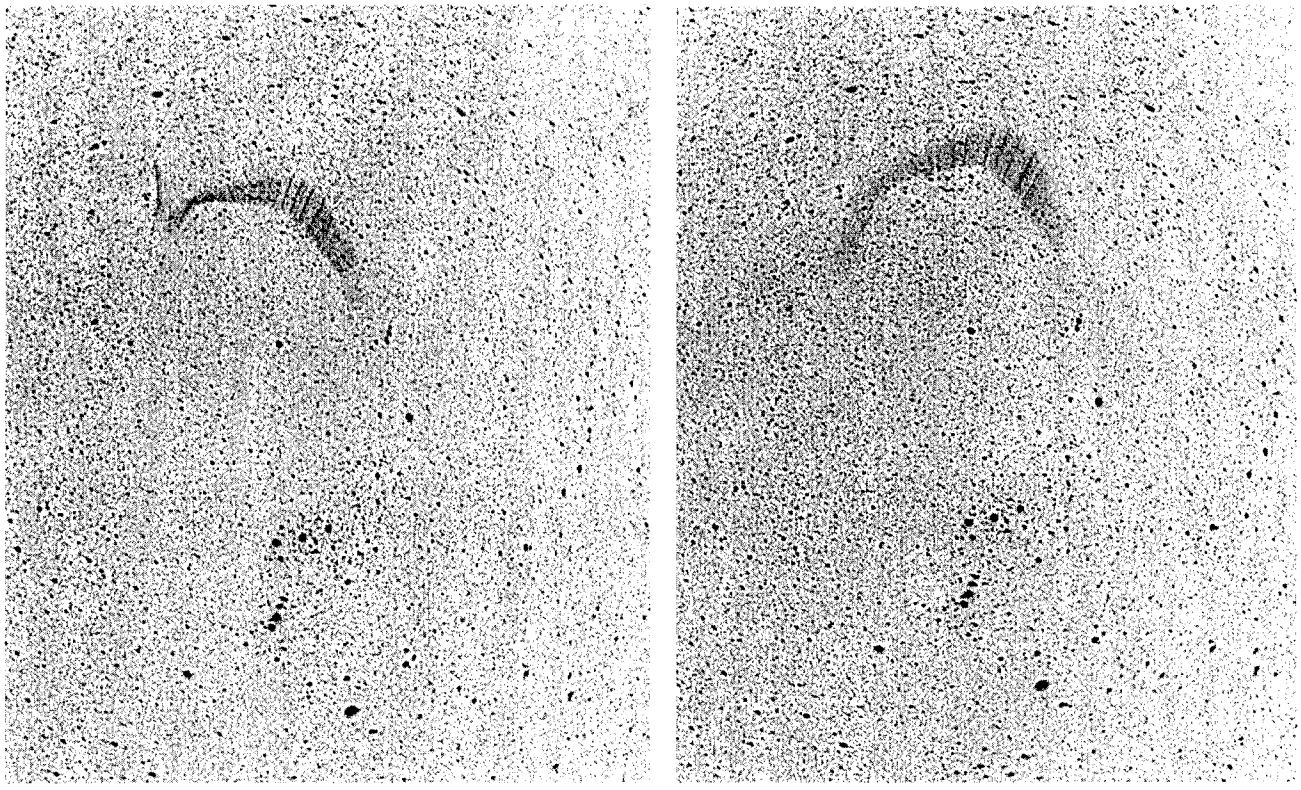

Figure 5 – Persistent train reported by Carlos Mas Clemente from El Pinar de Santiago (Gran Canaria, Spain). Objective 24 mm, f/2.5 and Tmax 3200 ISO. *Left:* exposed from 03:09:30 UT to 03:10:30 UT. *Right:* exposed from 03:11:30UT to 03:12:30 UT on November 17.

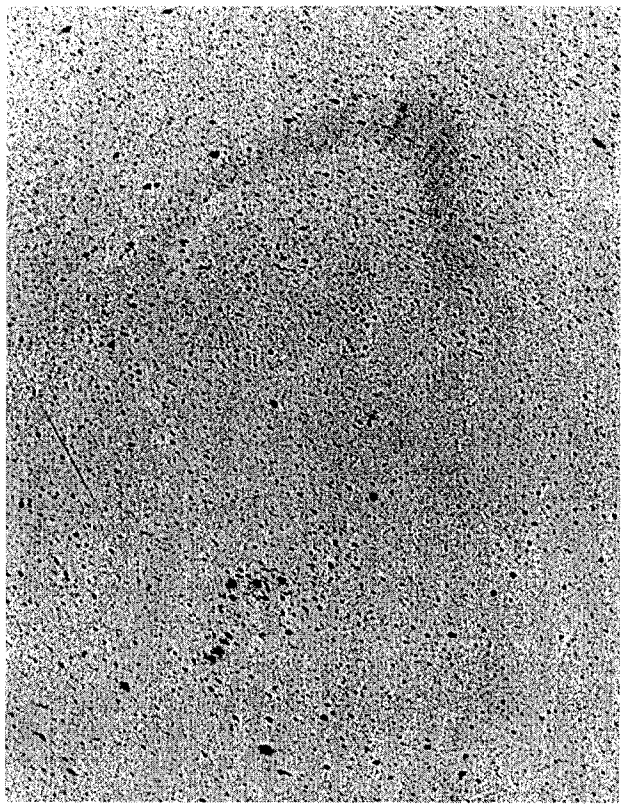

Figure 6 – The same persistent train as in Figure 5 exposed from 03:13:30 UT to 03:14:30 UT on November 17.

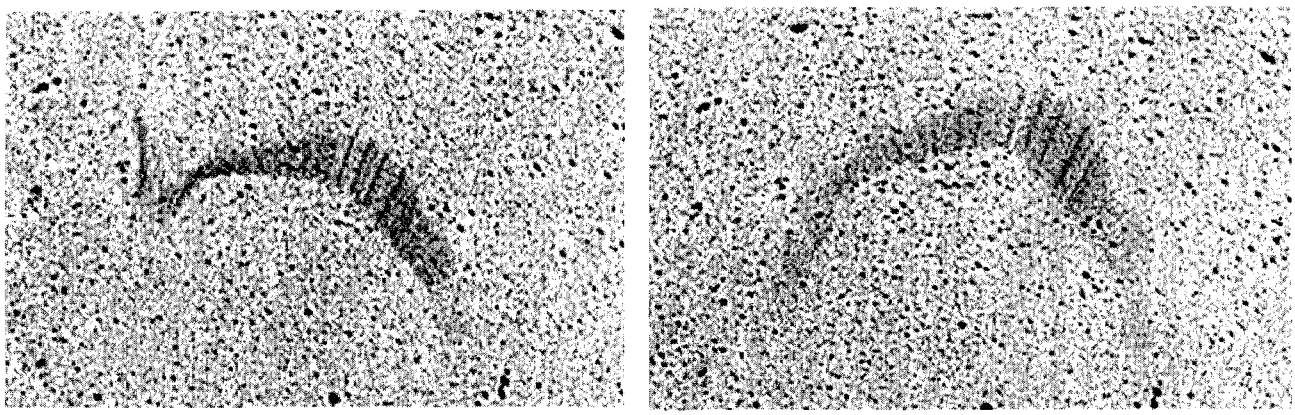

Figure 7 – Enlargements of the diffusion structures of the persistent train in Figure 5.

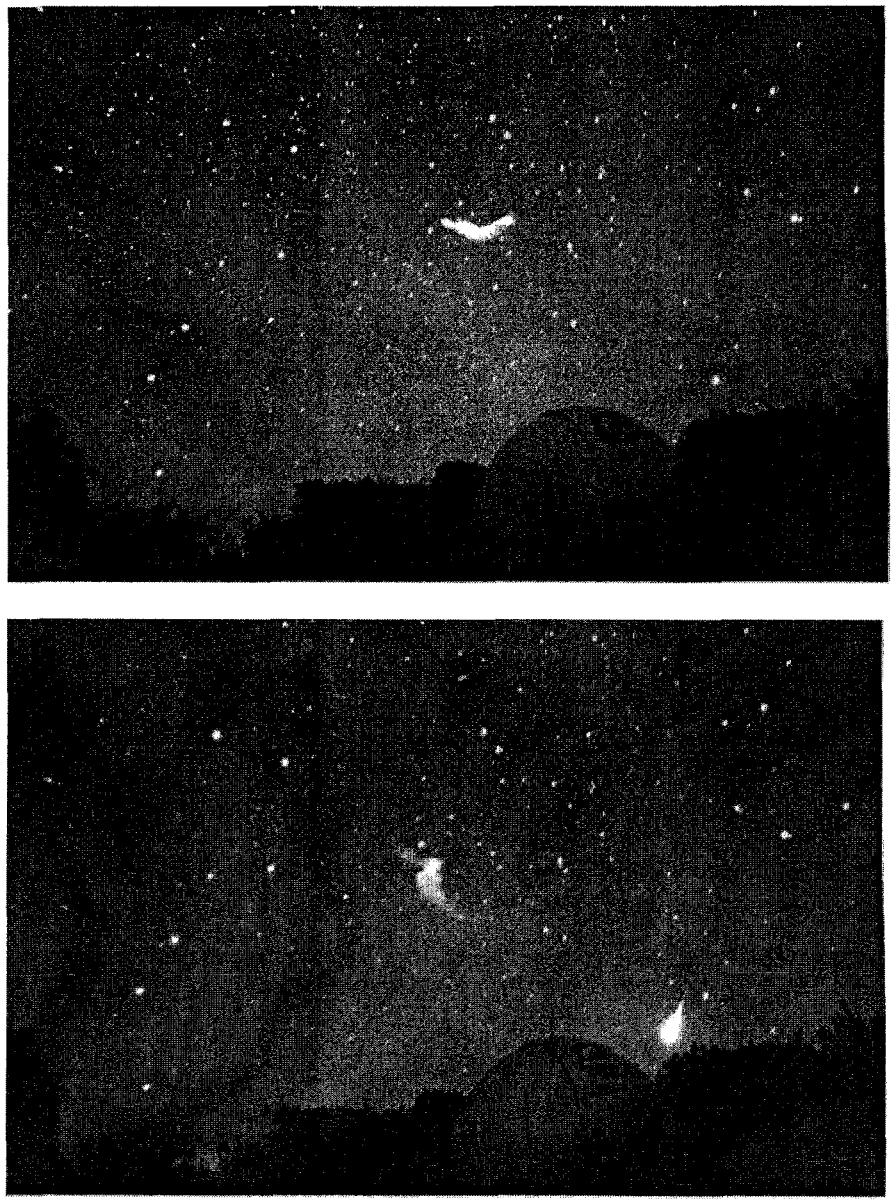

Figure 8 – Persistent train near Ursa Major area from Mallorca island taken by Grupo UMA from Observatorio Astronómico de Mallorca. At right, the persistent train and a new fireball. Tmax 3200 ISO, 50 mm, f/2.8. exposure times are from 01:26:14 to 01:27:25 UT (*top*) and from 01:32:16 to 01:33:24 UT (*bottom*) on November 17.

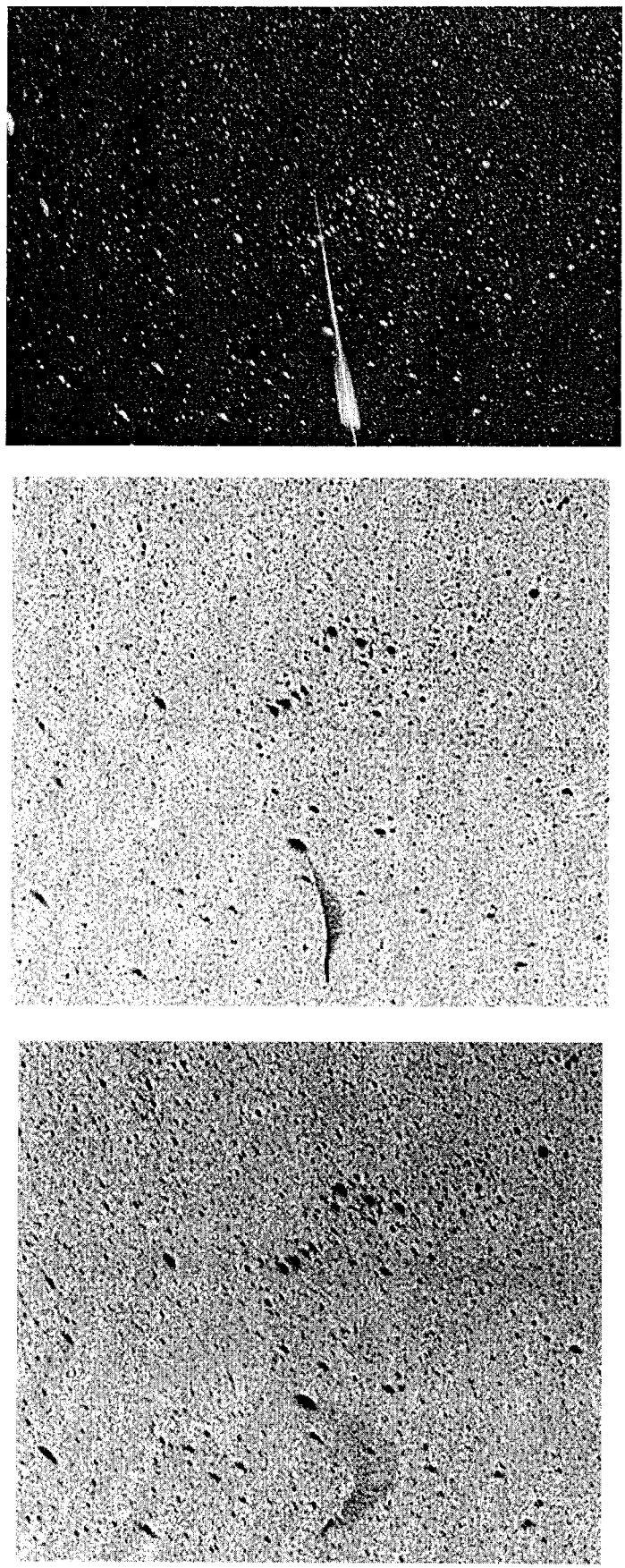

Figure 9 – Fireball in Lepus and its persistent train with a minute expositions between 04:30:30 to 04:35:30 UT on November 17.

Here we would like to present some pictures of different persistent trains from 1998 observations. Not many data are available for 1999 and 2000, and the photographs taken are poor. One event was registered though on 30 different negatives. It was persisting for 45 minutes.

References

[1] Luis R. Bellot Rubio, "On the Presence of trains in Meteor Showers", *WGN* 20:3, 1992, pp. 140–144.

[2] Orlando Benítez Sánchez, "Campaña de Observación Leonidas 1998–99: Análisis de las observaciones españolas de bólidos.", *Meteors, Revista de la Sociedad de Observadores de Meteoros y Cometas de España* Nr. 12, pp. 18–30.

[3] "Resultados fotográficos de las Leónidas de 1998", *Revista Universo* Nr. 47, March 1999, pp. 28–34.

[4] W.J. Baggaley, C.H. Cummack, "The duration of long-lived meteor trains", *Bull. Astron. Inst. Czechosl.* 30 (1979), pp. 180–183.

[5] S. Molau, V. Gerhardt, "Spectacular Leonid Fireball", *WGN* 25:1, 1997, pp. 54–56.

[6] Y. Shigeno, M. Toda, M. Kobayashi, "A Spiral Meteor Train", *WGN* 26:5 1998, pp. 220–225.

[7] J. Rajchl, "About turbulence and attachment in meteor trains", *Bull. Astron. Inst. Czechosl.* 20 (1969, Nr. I), pp. 10–13.

Author's address

Orlando Benítez Sánchez, Urb. El Pilar, Ptal. 20, 4°A, E-35012 Las Palmas de Gran Canaria, Spain, benor@navegalia.com

The 2001 Leonids by the Radio Meteor Observing Network in Japan

Hiroshi Ogawa, Shinji Toyomasu, Kouji Ohnishi, Kimio Maegawa, Shinobu Amikura, Takashi Asahina, and Kayo Miyao

On November 18, 2001, the Leonid meteor storm appeared over Japan. To measure the Leonid activity in 2001, radio meteor observations of 77 sites in Japan started the monitoring campaign on November 1. On November 15 and 17 in the UT evening, many long echoes were observed. On November 18 in the UT evening, we caught the Leonid meteor storm activity by radio. Around the peak time, however, it became impossible to count the number of echoes because the number of long echoes increased. Therefore, we estimated the Leonid activity by analyzing a "reflection time" of meteor echoes. As a result, we found a clear main peak (18^h20^m–18^h30^m UT on November 18) and a sub-peak (21^h20^m–21^h30^m UT) of the storm. This main peak is due to the components of the 9-revolution (1699) and 4-revolution (1866) dust trails, and the sub peak is probably due to components not computed. And we also found that the fireball activity was nearly constant in time around the storm. Therefore, this fireball component is probably another component different from those which produced the main and sub-peak.

1. Introduction

In November 2001, the Leonid meteor shower showed a great appearance over America, Asia and Australia [1]. In Japan, many observers encountered the Leonids' main peak around 18^h13^m UT on November 18, and many reports also show that the main peak remained for a long time. Radio meteor observations observed a sub-peak around 22^h UT on November 18 [2]. The fireball report based on visual observations in Japan showed that fireballs were more active on November 15 and 17 (UT) than on November 16th (UT) [3,4].

In Japan, many radio meteor observers monitored the Leonid meteor activity. In 2001, 77 observational stations participated in the "Leonids 2001 project by radio meteor observations all over the world" [5]. Participants started to monitor the whole Leonid meteor activity. This project succeeded in monitoring and observing the Leonid activity.

Since November 1, observers monitored the meteor activity, and the background level was defined. On November 15 in the UT evening, many long echoes were observed, and this is an unpredicted appearance. On November 17 in the UT evening, many echoes and long echoes were observed, too. Around the main peak, however, it became impossible to count the number of meteor echoes because the number of long echoes increased. Therefore, we have to analyze these data by using another method. In this research, we estimated the Leonid activity around the main peak by using the "Reflection Time". As a result, a complex peak structure was found.

2. Japanese radio meteor observation

Kazuhiro Suzuki et al. started the Japanese radio meteor observations in 1971, by receiving the signal from an FM broadcast station. Recently, however, it became difficult to use FM radio waves because of the increase of FM broadcast stations. Then, a new forward-scatter observation technique has been used since 1996 [6]. This is called Ham-band radio observing (HRO). HRO has become the major method for Japanese radio meteor observations. The transmitting station is the Fukui National College of Technology (Fukui, Japan). The frequency is 53.750 MHz with a 50-W continuous wave beacon. This method caught many meteor showers and outbursts [6,7]. At the receiving station, observers use a software running under the Windows operating system, and observe the meteor activity. This software was developed by Kazuhiko Ohkawa. The program analyzes the radio sound by Fast Fourier Transform (FFT) every half second, and one image file is produced every 10 minutes. Figure 1 is an example figure of this software. In 2001, there were 77 Japanese receiving stations in the "Leonid 2001 project by radio meteor

observations all over the world". Figure 2 is the observed image file around the peak. We could not count the number of echoes. Figure 1 shows the activity near 15^h00^m UT on November 18, and Figure 2 shows the activity near 18^h20^m UT.

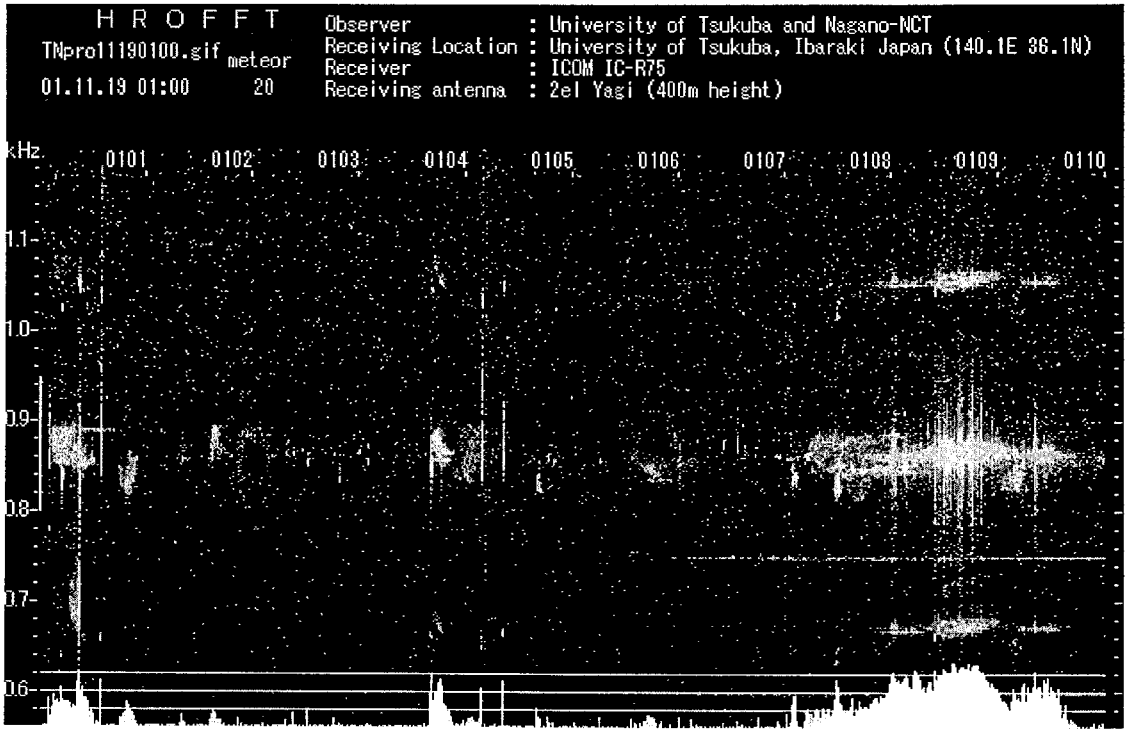

Figure 1 – The image file produced by the HROFFT software (University of Tsukuba).

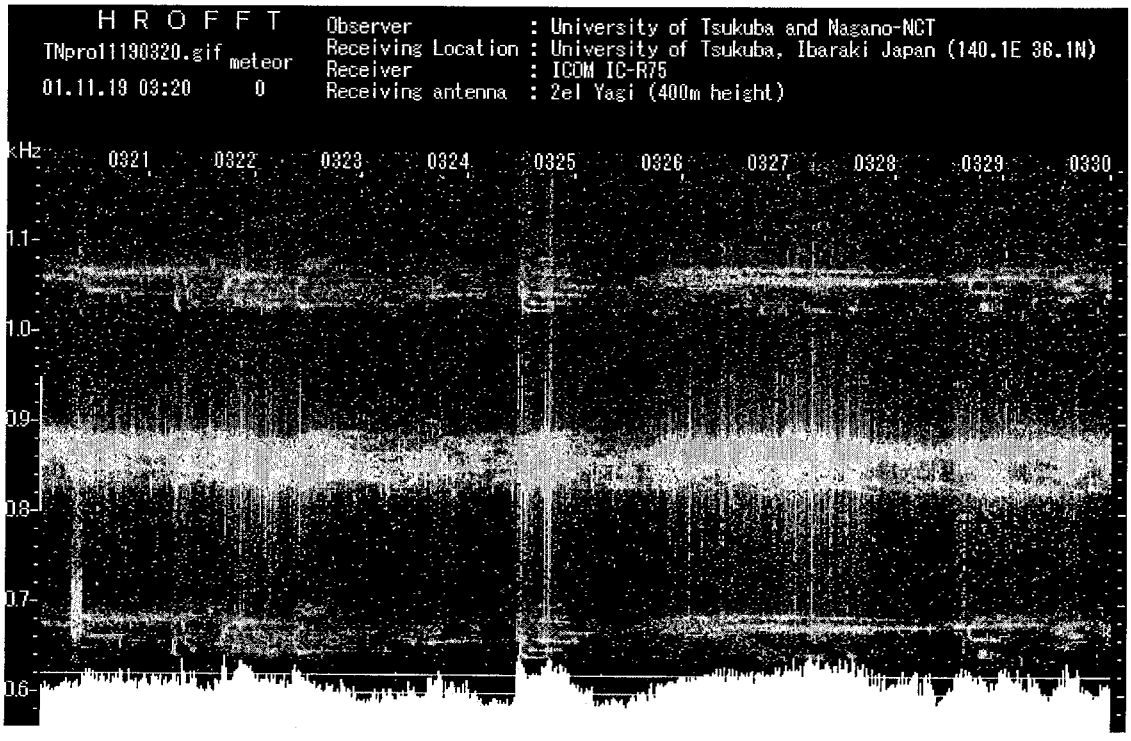

Figure 2 – The image file around the main peak of the Leonids (University of Tsukuba).

3. Reflection time

Around the main peak, it became impossible to count the number of echoes because the number of long echoes increased. Therefore, this research analyzed the FFT image files. These files contain data about the intensity of the meteor echoes. This research analyzes the total time of meteor echoes with the intensity over 10, 20, 30, and 40 dB. The intensity of 10 dB corresponds to 10^{-15}–10^{-16} W. Therefore, An echo over 30 or 40 dB corresponds to a bright meteor like a fireball. Figure 3 shows the result based on the reflection time for the 2001 Perseids. The result is similar to that of visual observations.

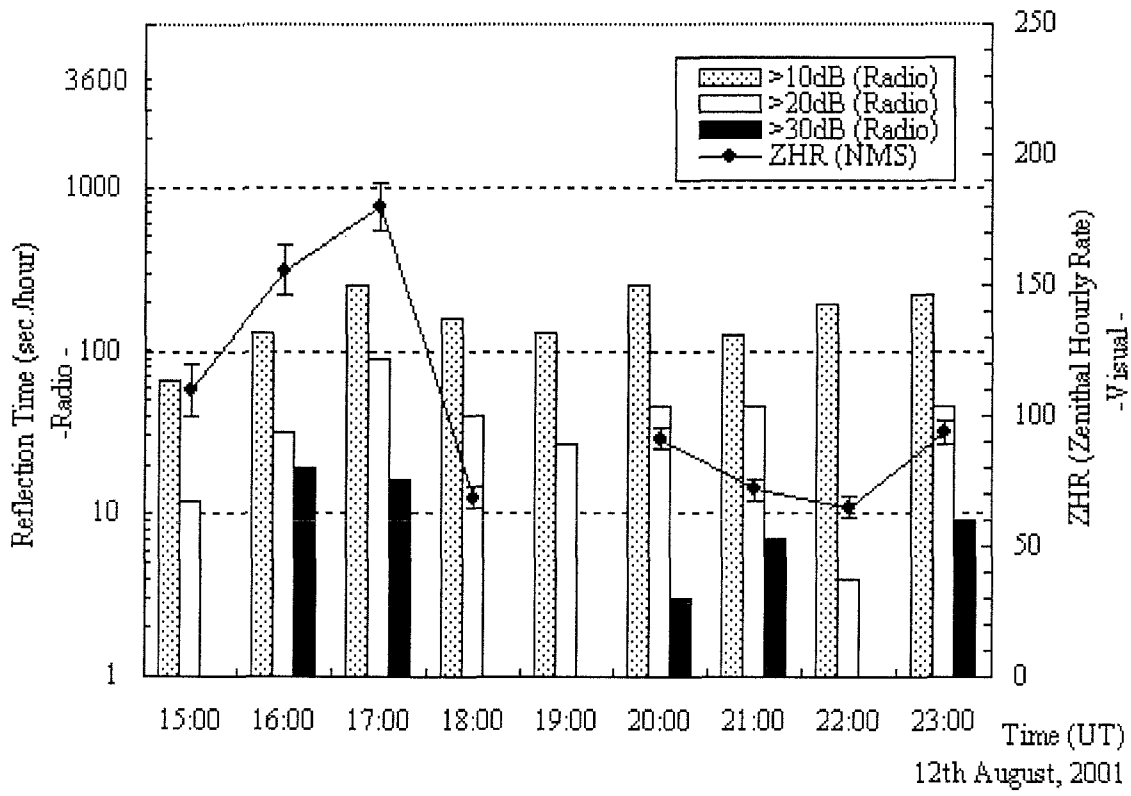

Figure 3 – The result based on the reflection time for the 2001 Perseids. (Radio: Misato Observatory, Wakayama, Japan; Visual: The Nippon Meteor Society [8])

The Leonid activity was estimated from the reflection time. Also, since the meteor echoes over 30 dB show represent the fireball component, we investigate the fireball activity from November 15 to November 18 (UT). This study uses 23 sites data from November 14–22. Data of November 14 and from November 20–22 defined the background level.

4. Results

Figure 4 is the result of the reflection time of echoes over 20 dB and 30 dB from 23 Japanese observational sites every 10 minutes.

From the curve of the reflection time over 20-dB echoes, one clear main peak and one clear sub-peak were found. The main peak was around $18^{h}20^{m}$–$18^{h}30^{m}$ UT on November 18, which corresponds to the main peak by visual techniques. The sub-peak was around $21^{h}20^{m}$–$21^{h}30^{m}$ UT on November 18. The half-width time of the main peak was about -90 min/ $+100$ min. The sub-peak width was about -45 min/ $+40$ min. In addition, the curve of the reflection time over

20 dB also shows some small peaks. Since these peaks were very sharp, it was possible only to observe one big meteor like a fireball. The graph of the reflection time over 30 dB intensity shows the bright-meteor component made of fireballs. This curve also shows that the fireball component was constant during the Leonid peak.

Data from November 15 to 17 (UT) were analyzed by the same method. Figure 5 shows the reflection time results over 20 dB from November 15 to 17 (UT) every five minutes. From the reflection time results (Figure 5), the bright-meteor component increased in the evening hours (UT) of November 15 and 17. On November 16 in the UT evening, there were relatively few bright meteors. This is a result similar to visual observations [3,4]. Therefore, there is the possibility of an encounter with an unknown dust trail.

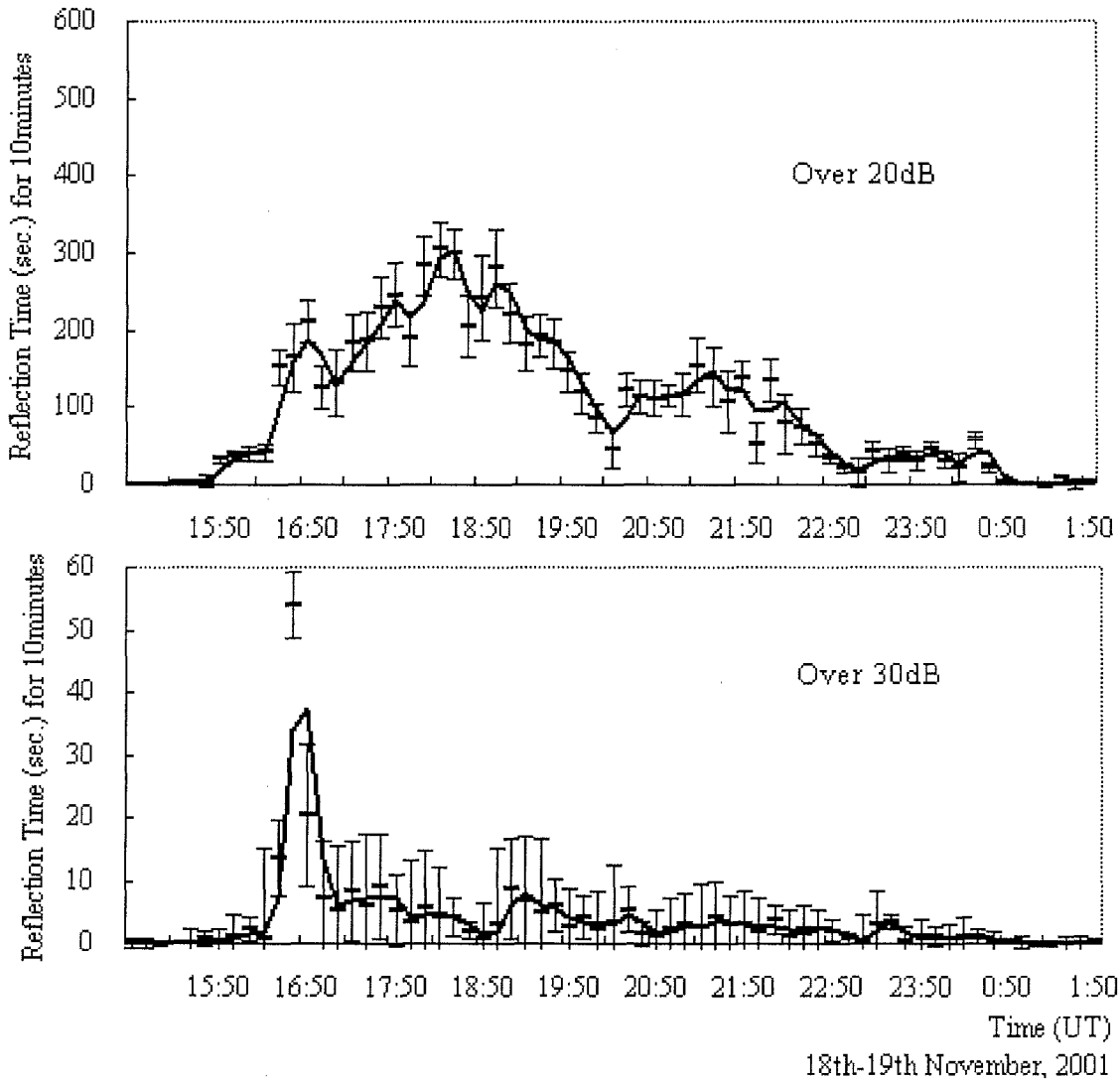

Figure 4 – The reflection time analysis of echoes over 20 dB and 30 dB every 10 minutes. The observers are as follows: Takashi Asahina, Isamu Ohmori, Yoichi Okamoto, Natsuko Ganzawa, Kazuhisa Kageyama, Takumi Yata, Masayuki Yamamoto, Taisuke Kondo, Kouji Ohnishi, Yosuke Utsumi, Yoshiharu Ito, Kayo Miyao, Kazuyuki Nagao, Seiji Fukushima, Masayuki Kobayashi, Kimihiro Norizawa, Minoru Ehara, hitoshi Yadotani, Hoshino girls' High School, Misato Observatory, Okayama-Asahi High School, Awa Highschool Amateur Radio Club JA5YGJ, University of Tsukuba.

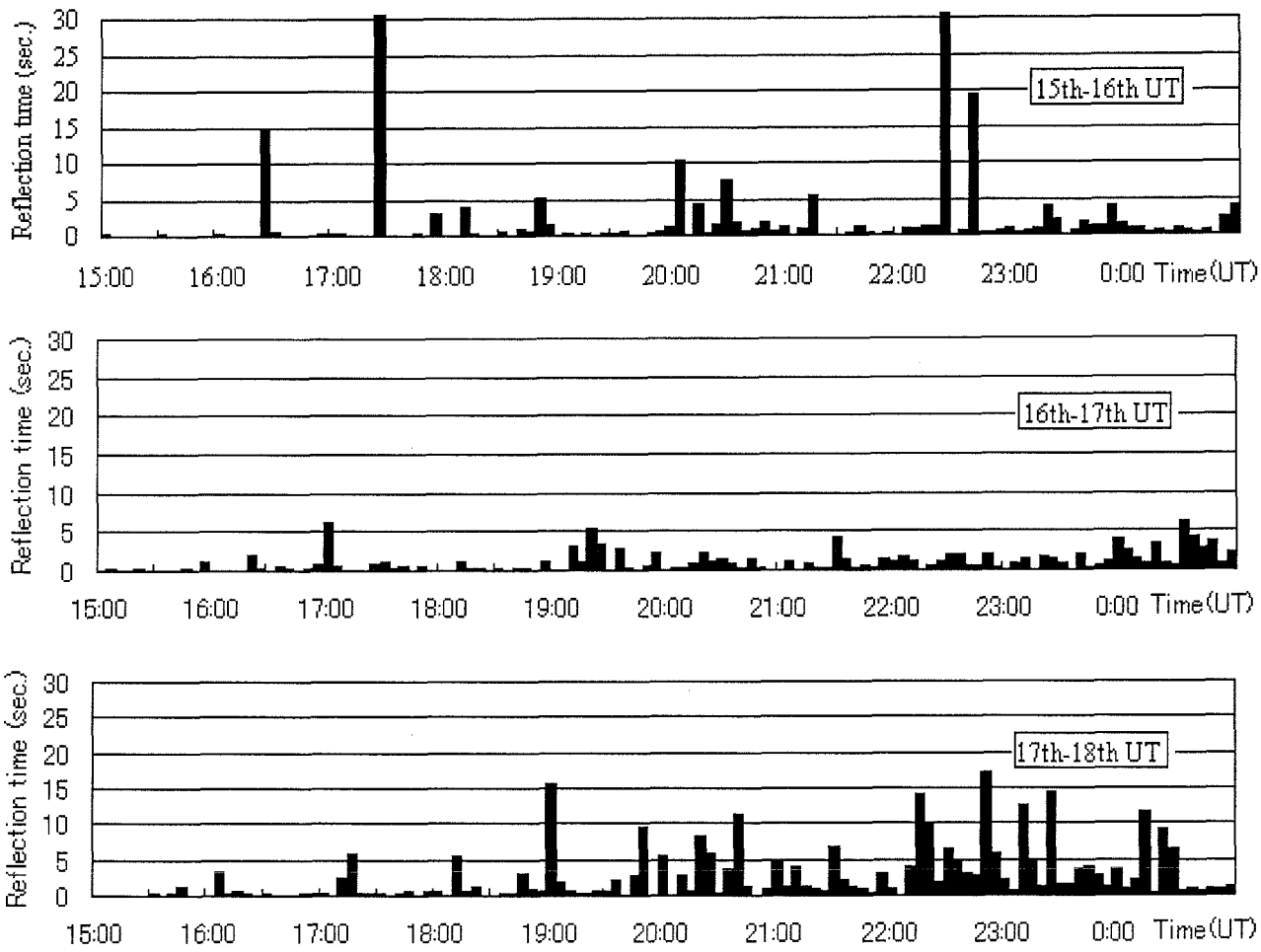

Figure 5 – The reflection time analysis from November 15 to 17 every five minutes. Observers are as follows (15 sites): Takashi Asahina, Isamu Ohmori, Kazuhisa Kageyama, Takumi Yata, Kouji Ohnishi, Yosuke Utsumi, Kazuyuki Nagao, Hitoshi Yadotani, Kimihiro Norizawa, Minoru Ehara, Hoshino girls' High School, Misato Observatory, Okayama-Asahi High School, Awa Highschool Amateur Radio Club JA5YGJ, University of Tsukuba.

5. Discussion

From Japanese radio meteor observational data, we found one clear main peak and one clear sub-peak in the Asian-Australian peak (around 18^h UT on November 18). The main peak was 18^h20^m–18^h30^m UT on November 18 ($\lambda_\odot = 237°.094$–$237°.101$), the sub-peak was 21^h20^m–21^h30^m UT on November 18 ($\lambda_\odot = 237°.221$–$237°.228$). The length on the dust trail passage is estimated for the main peak to be $9.68 \pm 0.96 \times 10^4$km and for the sub-peak to be $4.63 \pm 1.01 \times 10^4$km. However, the sub-peak at 21^h20^m–21^h30^m UT was unpredicted by some researchers [9–11]. Since there were few visual observations, this peak cannot be compared with visual results. However, there were many reports of some meteors in the twilight sky. In addition, this sub-peak was observed at almost all of the radio observing sites in Japan. On the other hand, the curve of the reflection time over 30 dB showed a bright-meteor component probably from fireballs. Figure 3 shows that the level of the fireball component was constant during the peak. This has already been analyzed from visual observational data, which is the constancy of meteors brighter than magnitude -1 [2]. This means the fireball component was not included in main and sub-peak components and there was another component for bright meteors. Therefore, the 2001 Leonid activity around the Asian and Australian peak has three components; (1) the main

peak component, (2) the sub-peak component which was unpredicted, and (3) the bright-meteor component.

Figure 4 and Figure 5 do not only show the fireball activity, but also the appearance time of the fireballs. The comparisons from 15^h00^m–20^h00^m UT on November 15, 16, and 17 are shown Table 1. Data of radio meteor observations were analyzed every one minute.

Table 1 – Comparison of fireball appearance times between visual and radio from November 15 to 17 Visual: The Nippon Meteor Society (the number means the magnitude of the fireball and V: visual, T: TV observation); Radio: same stations as in Figure 3, (15 sites, "(20)" and "(30)" indicate the peak of duration time over 20 dB or 30 dB. "(30)" includes "(20)").

November 15 (UT)		November 16 (UT)		November 17 (UT)	
Radio	Visual	Radio	Visual	Radio	Visual
	15:02:55 (−3V)		18:33 (−4V)		15:35:26 (−3V)
16:28 (20)	16:27:59 (−4T)	18:55 (20)		16:07 (20)	
16:37 (20)	16:37:29 (−3V)	19:14 (20)	19:14:44(−3V)	17:14 (30)	
17:02 (20)		19:24 (20)		18:10 (20)	
17:26 (30)	17:26 (−3V)				18:37:41 (−3V)
17:56 (20)				19:04 (20)	19:04 (−4V)
	18:13:50 (−4V)			19:38 (20)	
18:14 (20)	18:14:01 (−3T)			19:46 (20)	19:45 (−4V)
18:44 (20)				19:50 (20)	19:49 (−4V)
18:52 (30)					19:56 (−4V)
	19:11 (−3V)				
19:33 (20)	19:33 (−8V)				

Almost all of the peaks in the reflection time in the radio data correspond to the appearance times of fireballs in visual data. Therefore, we could estimate when the fireballs appeared.

6. Conclusion

In this study, we obtained information about the peak structure, fireball component, and appearance times of fireballs using the reflection time. In particular, some unpredicted activities were observed, which were the 21^h20^m–21^h30^m UT peak on November 18 and many fireballs (long echoes) on November 15 and 17 (UT). From these results, consequently, the structure and character of the 2001 Leonids were clarified, and we now need to discuss in detail why these additional features occurred.

References

[1] R. Arlt, J. Kac, V. Krumov, A. Buchmann, J. Verbert, "Bulletin 17 of the International Leonids watch: First Global Analysis of the 2001 Leonids Storms", *WGN* 29 (2001), pp. 187–194.

[2] H. Ogawa, S. Uchiyama , "The 2001 Leonids Meteor Storm over Japan", *WGN* 29 (2001), pp. 206–213.

[3] Y. Shiba, "The Reports of Fireball Observations 96", *The Astronomical Circular of The Nippon Meteor Society* 714 (2002), p. 7.

[4] Y. Shiba, "The Reports of Fireball Observations 97", *The Astronomical Circular of The Nippon Meteor Society* 715 (2002), pp. 24–29.

[5] H. Ogawa, S. Toyomasu, K. Ohnishi, K. Maegawa, "Leonids 2001 Project by Radio Meteor Observation All Over The World", `http://homepage2.nifty.com/~baron/`, 2001.

[6] K. Maegawa, "HRO: A New Forward-Scatter Observation Method Using a Ham-Band Beacon", *WGN* 27 (1999), pp. 64–72.

[7] K. Maegawa, M. Ueda, Y. Minagawa, "HRO Caught Outburst on June 27, 1998", *WGN* 27 (1999), pp. 76–80.

[8] The Nippon Meteor Society, "Perseids 2001", `http://www.nms.gr.jp/en/`, 2001.

[9] E.J. Lyytinen, "Prediction the strength of Leonids outburst", *Earth, Moon, and Planets* 82 (2000), pp. 149–166.

[10] E.J. Lyytinen, M. Nissinen, T. van Flandern , "Improved 2001 Leonids Storm Predictions from a Refined Model", *WGN* 29 (2001), pp. 110–118.

[11] R.H. McNaught, D.J. Asher, "Leonids dust trails and meteor storms", *WGN* 27 (1999), pp. 85–102.

Author's address

Hiroshi Ogawa, The Nippon Meteor Society, 36-47 Nakane, Kutsukake, Toyoake, Aichi, 470-1101, Japan, e-mail `ogawa@nms.gr.jp`.

Shinji Toyomasu, Misato Observatory, 180 Matsugamine, Misato, Kaiso, Wakayama, Japan, e-mail `toyomasu@obs.misato.wakayama.jp`.

Kouji Ohnishi, Nagano National College of Technology, 716 Tokuma, Nagano, Nagano, 381-8550, Japan, e-mail `ohnishi@ge.nagano-nct.ac.jp`.

Kimio Maegawa, Fukui National College of Technology, Geshi, Sabae, Fukui, 916-8507, Japan, e-mail `kmaegawa@fukui-nct.ac.jp`.

Shinobu Amikura, University of Tsukuba, 201 Kakehi, 3-12-9 Amakubo, Tsukuba, Ibaraki, 305-0005, Japan, e-mail `shino1@mw.tramonline.net`.

Takashi Asahina, Hiroshima University, 9-308, 2-812-62 Kagamiyama, Higashi-Hiroshima, Hiroshima, 739-0046, Japan, e-mail `n_asahi@mvd.biglobe.ne.jp`.

Kayo Miyao, Asahigaoka High School, 3-4-3 Daimachi, Showa, Nagoya, Aichi, 466-0033, Japan, e-mail `kayo@dog.interq.or.jp`.

Radio Observations of the 2002 Lyrids and Eta Aquarids

R.B. Minton

An FM Radio Meteor System (FMRMS) was used to observe the Lyrids on April 22–23 and the η-Aquarids on May 2–10. This receiver has operated continuously since November 13, 2001, and also recorded the Leonids, Geminids, and Quadrantids [1]. The data are withdrawn and analyzed every 29 days, and Figure 1 shows the most recent interval from April 12 to May 10. All meteor showers have been recorded with a vertical 1/4-wave ground-plane antenna at frequency of 92.9 MHz.

The top half of Figure 1 is the raw count data, and the lower is raw counts minus the diurnal background count—I call this the residuals. The counts are stored every 6 minutes, and five such counts are plotted as one data value—a 30-minute sum. Ten days are shown on each line, except the third line which is 9 days followed by the diurnal average. The diurnal background is cyclic with a minimum meteor count near 6 pm, and a maximum near 6 am local time. Subtracting the background count aids in identifying real meteoric events that maybe near the threshold of detection. The FMRMS software sums and averages the diurnal background count with provisions to exclude any dates that have abnormal counts due to meteor showers or noise.

The residuals have equal positive and negative values for the entire 29 day interval. Positive residuals represent counts in excess of the average, and negative less. The η-Aquarids are evident from May 2 to 10 as the positive excess above the x-axis (time). The y-axis is radio counts per 30 minutes with each vertical dash representing 50 counts.

When the shower counts are well above the diurnal background (and the radiant is above about 45° altitude); a peculiar signature is observed. The data reveal a double peak with a central minimum coinciding with the radiant crossing the observer's local meridian. The zenithal hourly rate increases as the radiant rises, but the received power to the receiver from each meteor trail decreases as the aspect of the trail becomes more vertical. This is due to the scattered radiation of the meteor trail being maximum broadside to the trail, and almost zero in the trail direction. Meteor trails on the horizon are broadside, but they contribute little single due to their great distance. This double peak has now been observed in five meteor showers. In the η-Aquarids, there is a central minimum on May 5 and May 6 near $14^{h}30^{m}$ UT. At this time, the radiant was at an altitude of 51° and an hour angle 0:00. In the Lyrids, a minimum occurs on April 22 near $11^{h}30^{m}$ UT with the radiant altitude at 83°, and an hour angle of 0:25 (+=W).

Table 1 – Radio counts in 30-minute sums of the Lyrids and the η-Aquarids.

Meteor Shower	UT Date	$\lambda_{\odot}$	Radio Counts
Lyrids	April 22	32°.0	50
	April 23	33°.0	30
η-Aquarids	May 2	43°.0	40
	May 3	43°.0	60
	May 4	44°.0	60
	May 5	45°.0	125
	May 6	46°.0	75
	May 7	47°.0	65
	May 8	48°.0	70
	May 9	49°.0	80
	May 10	50°.0	50

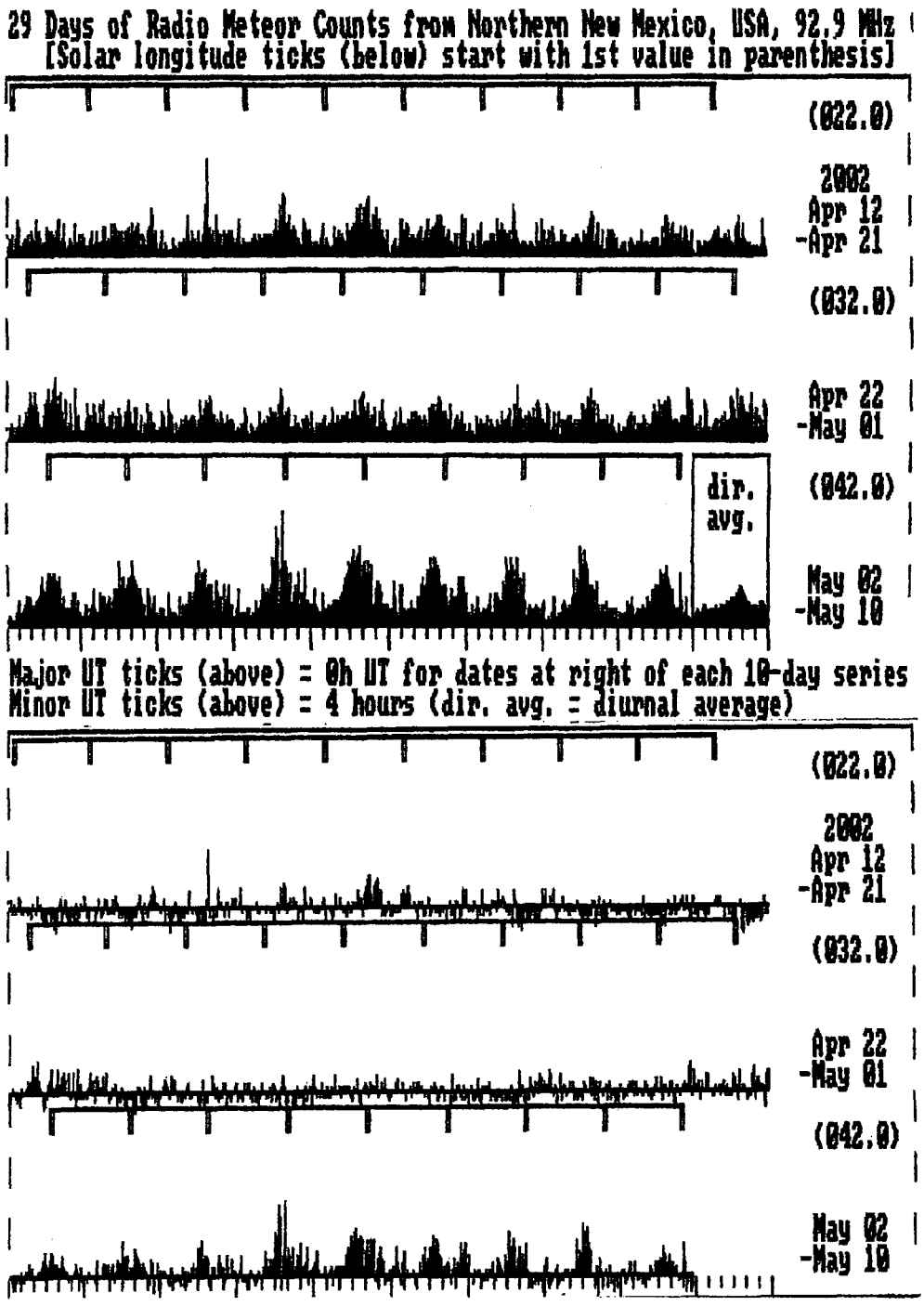

Figure 1 – Twenty-nine days of radio meteor counts from Northern New Mexico, USA, at 92.9 MHz.

Radio counts cannot be compared with visual counts. The Table 1 presents the maximum radio counts that are in excess of the expected diurnal background, i.e., radio counts attributable to the meteor shower itself. The UT dates are tick below the radio counts, and the solar longitudes are ticks above the radio counts.

References

[1] R.B. Minton, R.D. Lunsford, "Count Meteors with FM Radios", submitted for publication in *JALPO*, March 2002.

Author's address

R.B. Minton, 568 North First Street, Raton, NM 87740, USA.

The International Meteor Organization

Council

President: Jürgen Rendtel, Seestraße 6, D-14476 Marquardt, *Germany*,
tel. +49 (33208) 50753, e-mail: president@imo.net

Vice-Pres.: Alastair McBeath, 12A Prior's Walk, Morpeth, Northumberld. NE61 2RF, *Engl.*,
tel. +44 (1670) 518 487, email: vice_president@imo.net

Secretary-General: Robert Lunsford, Vance Street 161, Chula Vista, *CA 91910, USA*
tel. +1 (619) 585 9642, e-mail secretary@imo.net

Treasurer: Ina Rendtel, Mehlbeerenweg 5, D-14469 Potsdam, *Germany*,
tel. +49 (331) 520 707, e-mail: treasurer@imo.net
postal (giro) account number: 5472 34-107
bank code: 100 100 10 Postbank Berlin
(bank code and postbank to be mentioned together with account number!)

Other council members:
Rainer Arlt, Friedenstraße 5, D-14109 Berlin, *Germany*
Marc Gyssens, Heerbaan 74, B-2530 Boechout, *Belgium*
André Knöfel, Saarbrücker Straße 8, D-40476 Düsseldorf, *Germany*
Sirko Molau, Verbindungsweg 7, D-15366 Hönow, *Germany*
Mihaela Triglav, Podkraj 10 c, SLO-3320 Velenje, *Slovenia*

Commission Directors

Visual Commission: Rainer Arlt, e-mail: visual@imo.net

Telescopic Commission: M. Currie, 660, N'Aohoku Place, Hilo, *HI 96720, USA*,
e-mail: tele@imo.net

FIreball DAta Center: André Knöfel, e-mail: fidac@imo.net

Photographic Commission: Marc de Lignie, Prins Hendrikplein 42, NL-2264 SN Leidschendam,
the Netherlands, e-mail: photo@imo.net

Video Commission: Sirko Molau, e-mail: video@imo.net

Radio Commission: vacant, e-mail: radio@imo.net

WGN — The Journal of the International Meteor Organization and Observational Report Series

Editor-in-chief: Marc Gyssens, tel. 32 (477) 64 05 48, e-mail: wgn@imo.net
fax: 32 (11) 26 82 99 (mention "for Marc Gyssens")

Editorial board: R. Arlt, D. Asher, M. Beech, P. Brown, M. Currie, M. de Lignie, W. Elford, G. Kronk, R. Hawkes, D. Hughes, J. Jones, C. Keay, R. Koschack, A. McBeath, P. Pravec, J. Rendtel, M. Šimek, G. Spalding, I. Williams.

Typesetting: Urania, the Public Observatory of Antwerp

Web Site: http://www.imo.net

Do not miss it!

International Meteor Conference 2002

Frombork, Poland, September 26–29, 2002

Do not miss this unique opportunity to meet like-minded people! We anticipate that a lot of meteor enthusiasts from all over Europe and overseas will participate. Results on the 2001 Leonids and discussions on the 2002 Leonids may be expected. More information can be found at `www.imo.net/news/imc.html`.

The stock of the IMO

	EUR	USD
Publications in English:		
Photographic Meteor Data Base (1986)	4	4
Proceedings International Meteor Conference 1990	5	5
Proceedings International Meteor Conference 1991	5	5
Proceedings International Meteor Conference 1992	5	5
Proceedings International Meteor Conference 1993	5	5
Proceedings International Meteor Conference 1994	5	5
Proceedings International Meteor Conference 1995	5	5
Proceedings International Meteor Conference 1996	5	5
Proceedings International Meteor Conference 1998	6	6
Proceedings International Meteor Conference 1999	6	6
Proceedings International Meteor Conference 2000	6	6
Gnomonic Atlas Brno 2000.0	3	3
Photographic Astrometry + diskette	7	7
WGN Observational Report Series:		
Vols. 1–5 (1988–1992): Visual Observations, per vol.	8	8
Vol. 6 (1993): Vis. Obs. and Electrophonic Fireball Cat.	8	8
Vols. 7–8 (1994–1995): Visual Observations, per vol.	8	8
Vols. 9–12 (1996–1999): Visual Observations, per vol.	10	10
Backissues of the WGN Journal:		
Volumes 19–20 (1991–1994): complete, per volume:	10	10
Volumes 23–29 (1995–2001): complete, per volume:	18	18